

# RESIDUAL TRACKING AND STOPPING FOR ITERATIVE RANDOM SKETCHING\*

NATHANIEL PRITCHARD<sup>†</sup> AND VIVAK PATEL<sup>‡</sup>

**Abstract.** Iterative random sketching (IRS) offers a computationally expedient approach to solving linear systems. However, IRS’ benefits can only be realized if the procedure can be appropriately tracked and stopped—otherwise, the algorithm may stop before the desired accuracy is achieved, or it may run longer than necessary. Unfortunately, IRS solvers cannot access the residual norm without undermining their computational efficiency. While iterative random sketching solvers have access to noisy estimates of the residual, such estimates turn out to be insufficient to generate accurate estimates and confidence bounds for the true residual. Thus, in this work, we propose a moving average estimator for the system’s residual, and rigorously develop practical uncertainty sets for our estimator. We then demonstrate the accuracy of our methods on a number of linear systems problems.

**Key words.** random sketching, linear systems, iterative methods, residual estimation, stopping criterion

**AMS subject classifications.** 65F10, 65F25, 60F10, 62L12

**1. Introduction.** Random sketching is cementing itself as a key tool in solving linear systems owing to its ability to generically approximate large linear systems of equations by smaller, more tractable systems of linear equations, thereby allowing for the efficient calculation of an approximate solution. Moreover, by applying random sketching repeatedly, the quality of these approximations can be improved [10], and such iterative random sketching (IRS) methods now enjoy a unified theory [5, 11]. Despite these important methodological and theoretical achievements, IRS methods provide their computational benefits if the procedure can be appropriately tracked and stopped: an IRS method stopped before the desired accuracy is achieved has failed its purpose, while an IRS method stopped too late will incur excess computation. Unfortunately, IRS methods are typically applied to systems sufficiently large so as to render computing and tracking typical metrics of progress (e.g., the residual norm) computationally infeasible.

Focusing on the residual norm, a simple approach to address this challenge is to use the residual norm of the sketched system at a given iterate. Indeed, owing to the Johnson-Lindenstrauss lemma [7], the residual norm of the sketched system ought to well-approximate the residual norm of the original system with high probability. However, such an estimator of the residual norm is subject to two sources of variability that impede its reliability. First, the residual norm of the sketched system is already a noisy approximation of the residual norm of the original system. Moreover, the residual norm of the original system at a given iteration inherits the randomness of the underlying randomized algorithm. Owing to these two sources of variability, the residual norm of a sketched system stemming from an IRS solver may not reflect the actual behavior of the iterates and their residuals. Indeed, as seen in [Figure 1b](#), the residual norm of a sketched system (green) varies substantially relative to the absolute error of the iterates.

---

\*Submitted to the editors DATE.

**Funding:** Authors are supported by UW-Madison WARF Award AAD5914.

<sup>†</sup>Department of Statistics, University of Wisconsin - Madison ([npritchard@wisc.edu](mailto:npritchard@wisc.edu)).

<sup>‡</sup>Department of Statistics, University of Wisconsin - Madison ([vivak.patel@wisc.edu](mailto:vivak.patel@wisc.edu), [vivakpatel.org](http://vivakpatel.org)).

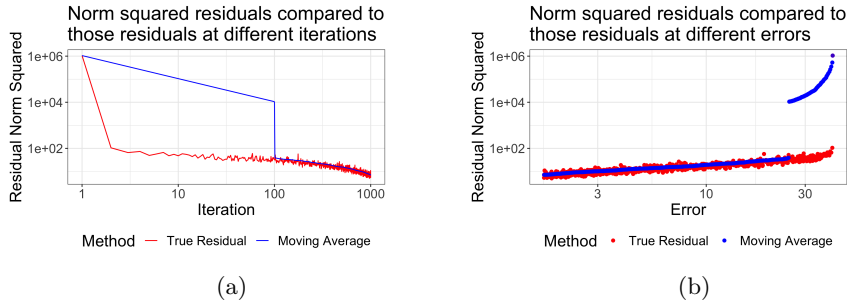


Fig. 1: Gaussian sketching was iteratively applied to solve a consistent system generated by the Moler matrix [13]. In (a), the residual norm-squared is compared to the iteration number. In (b), the residual norm-squared is compared with the absolute error. The red points are the residual-norm squared at the iteration, while the blue points are a moving average of the residual-norms squared with a width of 100.

Solutions to mitigate the effect of the underlying algorithm’s randomness include (1) using an average of the iterates and computing the residual norm of the averaged iterate for the sketched system; (2) using a moving average of the iterates and computing the residual norm of the moving average iterate for the sketched system; or (3) using a moving average of the residual norms. Unfortunately, using the average of the iterates would produce an error decay rate of  $\mathcal{O}(1/k)$  to overcome the bias induced by the initial iterate,<sup>1</sup> which is a tremendous slow down relative to the exponential convergence of IRS methods [5, 11]. Equally problematic, using a moving average of the iterates would require tracking as many solution-sized vectors as the width of the window in order to update the moving average, which would result in large memory requirements even for small-sized windows. As the most promising method of the three, a moving average of the residual norms requires only storing scalars—only as many as the size of the window—to update the moving average. Moreover, a moving average of the residual norms is a good reflection of the actual progress of the algorithm, an observation illuminated in Figure 1. Indeed, as seen in Figure 1, the moving average of the residual with a window of one hundred (blue) iterations is less variable than the instantaneous residual (red) and is a less variable estimate of the absolute error. Despite the benefits of the moving average of the residual norms, it too is infeasible to compute as it would require computing the residual norms, which we have already established require impractical computational costs.

However, the moving average of the residual norms can be estimated by using a moving average of the residual norms of the sketched systems. While using a moving average of the sketched residual norms to track the solver’s progress follows from a rather linear set of ideas, the moving average of the sketched residual norms has its own challenges. First, the moving average of the sketched residual norms continues to be a random quantity. This randomness raises the question: how well does the moving average of the sketched residual norms capture the moving average of the residual norms? A question whose answer demands that we derive appropriate uncertainty

<sup>1</sup>The initial iterate can be replaced by the first iterate at which the average starts being used, but this results in the same issue

sets and coverage probabilities of these uncertainty sets, which is an order of magnitude more difficult than just generating the moving average of the sketched residual norms (i.e., the uncertainty set of a point estimator is more difficult to estimate and characterize than the point estimator alone).

A further complication is that we have to choose between multiple types of uncertainty sets and corresponding coverage probabilities. Specifically, do we want (1) an uncertainty set that covers *all* possible independent runs of a given IRS with the same initialization and the same system with a given probability at a particular iterate, (2) an uncertainty set that covers the entire path (i.e., over all iterates) of a single run of an IRS with a given probability, or (3) an uncertainty set that covers a single iterate of a single run of an IRS with a given probability? Indeed, the third uncertainty set is the main workhorse for producing the preceding two uncertainty sets,<sup>2</sup> and is, in our view, the more useful because it specifies the uncertainty in the behavior of the current run of an IRS method at (roughly) the current iterate. For this reason, developing guarantees for the third uncertainty set, and its coverage probability is the more pressing challenge.

To summarize, rigorously developing an estimate of the moving average of the residual norms and an appropriate uncertainty set is nontrivial. To address this challenge, we rigorously establish an estimator of the moving average of the residual norms using a moving average of the sketched residual norms; we rigorously develop and characterize the third aforementioned uncertainty set and the coverage probability of this uncertainty set; and we demonstrate the effectiveness of these estimators for tracking the moving average of the residual norms on a large collection of linear systems.

The paper is organized as follows. In [section 2](#), we tabulate important notation. In [section 3](#), we specify the problem that we are solving, the algorithm used to solve this problem, our residual moving average estimator, our estimate of its uncertainty set, and our stopping condition. In [section 4](#), we rigorously establish the foundations of our estimators. In [section 5](#), we numerically demonstrate the effectiveness of our estimators. In [section 6](#), we conclude.

**2. Notation.** We use the following the notation in this work.

Symbol	Description
$A$	A matrix in $\mathbb{R}^{m \times n}$ .
$b$	A constant vector in $\mathbb{R}^m$ .
$S_k$	A random matrix in $\mathbb{R}^{m \times p}$ that satisfies the Johnson-Lindenstrauss property.
$B$	A symmetric positive definite matrix in $\mathbb{R}^{n \times n}$ .
$\ \cdot\ _2$	The standard Euclidean norm.
$\ y\ _B$	Equals $\sqrt{\langle y, By \rangle}$ where $y \in \mathbb{R}^n$ .
$\ D\ _B$	Equals $\max_{\ y\ _B=1} \sqrt{\langle Dy, BDy \rangle}$ where $D \in \mathbb{R}^{n \times n}$ .
$x_k$	The iterate at iteration $k$ .
$x^*$	A solution to $Ax = b$ .
$r_k$	The residual at iteration $k$ , i.e. $r_k = Ax_k - b$ .

<sup>2</sup>To produce the first uncertainty set and corresponding probability bounds, we need only take expectations in the derivation of the third uncertainty set. To produce the second uncertainty set and corresponding probability bounds, we need only take a union bound in the derivation of the third uncertainty set.

$\tilde{r}_k$	The sketched residual $S'_{k+1}r_k$ .
$\rho_k^\lambda$	The moving average of width $\lambda$ of sketched residuals norms squared.
$\iota_k^\lambda$	The moving average of width $\lambda$ of the sketched residual norms to the fourth power.
$\mathbf{SE}(\sigma^2, \omega)$	A sub-Exponential distribution with variance bounded by $\sigma^2$ and second parameter $\omega$ .
$d$	Used for moments of a distribution.
$\eta$	Constriction parameter used in interval width.
$Q_k$	Matrix with orthonormal columns.
$\tau_\ell$	Stopping time indicating iteration when $\text{span}\{\text{col}(Q_1), \text{col}(Q_2), \dots, \text{col}(Q_{\tau_\ell})\} = \text{row}(AB^{-1/2})$ .
$\xi_I$	User specified control on probability of stopping too late.
$\xi_{II}$	User specified control on probability of stopping too early.
$v$	User specified threshold for a small enough residual to warrant stopping.
$\mathbb{E}[\cdot]$	The expectation operator.
$\mathbb{P}(\cdot)$	The probability measure.
$\mathcal{F}_k$	The $\sigma$ -algebra generated by $S_1, \dots, S_k$

---

### 3. Problem Formulation & Algorithm.

We are interested in solving

$$(3.1) \quad Ax = b$$

where  $A \in \mathbb{R}^{m \times n}$  is the coefficient matrix;  $b \in \mathbb{R}^m$  is the constant vector; and we assume

ASSUMPTION 3.1. *The linear system, (3.1), is consistent.*

To solve (3.1), we will employ Iterative Random Sketching (IRS), which starts with an initial iterate  $x_0 \in \mathbb{R}^n$  and generates a sequence of iterates  $\{x_k : k \in \mathbb{N}\}$  according to

$$(3.2) \quad x_{k+1} = x_k - B^{-1}A'S_{k+1}(S'_{k+1}AB^{-1}A'S_{k+1})^\dagger S'_{k+1}(Ax_k - b),$$

where  $\{S_k \in \mathbb{R}^{m \times p} : k \in \mathbb{N}\}$  are independent random variables satisfying a minor variation of the Johnson-Lindenstrauss property [7], which is stated presently.

*Remark 3.2.* The update in (3.2) is a general update rule formulated and studied in [5, 11], and applies to IRS, randomized Gaussian pursuit, Randomized Kaczmarz, and Randomized Newton's methods. We focus only on the IRS case. Moreover, the actual IRS iteration is calculated differently from (3.2), but is mathematically equivalent.  $\blacksquare$

DEFINITION 3.3. *A matrix  $S \in \mathbb{R}^{m \times p}$  satisfies the Johnson-Lindenstrauss property if there exists constants  $C, \omega > 0$  for all  $\delta \geq 0$  and for any  $x \in \mathbb{R}^m$ ,*

$$(3.3) \quad \mathbb{P}(|\|S'x\|_2^2 - \|x\|_2^2| > \delta\|x\|_2^2) < 2e^{-\min\{Cp\delta^2, (Cp\delta)/\omega\}}.$$

In Definition 3.3, the constants  $C$  and  $\omega$  are determined by the way that  $\{S_k : k \in \mathbb{N}\}$  are generated, and there are many choices, such as sparse Rademacher matrices [1],

Table 2: Values of  $C$  and  $\omega$  in [Definition 3.3](#) for common sampling methods.

	$C$	$\omega$
Gaussian Matrix <a href="#">[3]</a>	0.23467	.1127
Achlioptas <a href="#">[1]</a>	0.23467	.1127
FJLT <a href="#">[2]</a>	0.03125	.0625

Sparse Hadamard Transform [\[2\]](#), and Gaussian matrices [\[3, 6, 8\]](#). For these examples, the values of  $C$  and  $\omega$  are supplied in [Table 2](#).

From a statistics perspective, [Definition 3.3](#) specifies a random variable whose distribution is in the family of sub-Exponential distributions. Sub-Exponential random variables can equivalently be defined by their moment generating function, as shown in Theorem 2.13 of [\[12\]](#) and [Lemma A.4](#). Importantly, sub-Exponential random variables are characterized by two parameters that control the variance,  $\sigma^2$ , and transition point from sub-Gaussian to sub-Exponential behavior,  $\omega$ , and are denoted by  $\mathbf{SE}(\sigma^2, \omega)$ .

**3.1. IRS Solver with Tracking and Stopping with a Fixed Moving Window.** As mentioned above, IRS, [\(3.2\)](#), can reduce the computational costs associated with approximately solving system [\(3.1\)](#), but these can only be realized if the progress of the IRS algorithm can be tracked and stopped in an inexpensive manner. To this end, we propose

1. a computationally-inexpensive and memory-efficient estimator and an equally inexpensive and efficient estimated  $(1 - \alpha)$ -credible interval for tracking the  $\lambda$ -moving average residual of the system,<sup>3</sup> where  $\lambda$  is the moving average window selected by the user, and  $\alpha \in (0, 1)$  is the user-specified probability that the credible interval fails to capture the residual;

2. and a stopping condition that controls the probability of failing to stop the procedure at a user-specified probability of  $\xi_I \in (0, 1)$ , and controls the probability of stopping the procedure too early at a user-specified probability of  $\xi_{II} \in (0, 1)$ .

The complete procedure is described in [Algorithm 3.1](#), and its components are described below.

*Point Estimator.* We propose the following point estimate of the moving average over the residual during iteration  $k$ :

$$(3.4) \quad \rho_k^\lambda := \sum_{i=k-\lambda+1}^k \frac{\|S'_{i+1}r_i\|_2^2}{\lambda} = \sum_{i=k-\lambda+1}^k \frac{\|\tilde{r}_i\|_2^2}{\lambda},$$

where  $r_i = Ax_i - b$ ;  $\tilde{r}_i = S'_{i+1}r_i$ ; and  $\lambda \in \mathbb{N}$  is a user defined moving average window. We note that  $\rho_k^\lambda$  can be updated from  $\rho_{k-1}^\lambda$  with  $\mathcal{O}(p)$  operations and  $\mathcal{O}(\lambda)$  storage given the update sketched residual,  $\tilde{r}_k$ , computation as part of [\(3.2\)](#). The consistency of [\(3.4\)](#) to the actual moving average is established in [Theorem 4.6](#).

<sup>3</sup>A  $(1 - \alpha)$ -credible interval is an interval in which the residual moving average is with probability  $(1 - \alpha)$ . An estimated  $(1 - \alpha)$ -credible interval is an interval that uses estimates of unknown values in the  $(1 - \alpha)$ -credible interval to compute a practical interval.

---

**Algorithm 3.1** Tracking and Stopping with a Fixed Moving Window
 

---

**Require:**  $A \in \mathbb{R}^{m \times n}$ ,  $b \in \mathbb{R}^m$ ,  $x_0 \in \mathbb{R}^n$

**Require:**  $\alpha, \xi_I, \xi_{II}, \delta_I \in (0, 1)$ ,  $\delta_{II} > 1$ ,  $\eta \geq 1, \nu$

**Require:** Random sketching method satisfying [Definition 3.3](#)

**Require:** Moving window size  $\lambda \in \mathbb{N}$

$k \leftarrow 0$

$\rho_0^\lambda \leftarrow 0$

$\iota_0^\lambda \leftarrow 0$

**while**  $k == 0$  **or** (3.9) fails to holds **do**

  # Iteration  $k$  #

  Generate  $(\tilde{A}_k, \tilde{b})$  from randomly sketch,  $S_{k+1}$ , and the original system,  $(A, b)$ .

$\tilde{r}_k = \tilde{A}_k x_k - \tilde{b}$

  Update moving average  $\rho_k^\lambda$  from  $\rho_{k-1}^\lambda$ ; see (3.4).

  Update fourth moment estimate  $\iota_k^\lambda$  from  $\iota_{k-1}^\lambda$ ; see (3.6).

  Update the estimated  $(1 - \alpha)$ -interval; see (3.5).

  Update iterate  $x_{k+1}$  from  $x_k$ ; see (3.2).

$k \leftarrow k + 1$

**end while**

**return**  $x_k$  **and** estimated  $(1 - \alpha)$ -interval

---

*Estimated Credible Interval.* We propose the estimated  $(1 - \alpha)$ -credible interval at iteration  $k$  over window  $\lambda$  to be

$$(3.5) \quad \rho_k^\lambda \pm \max \left( \sqrt{\frac{2 \log(2/\alpha) \iota_k^\lambda (1 + \log(\lambda))}{C p \lambda \eta}}, \frac{2 \log(2/\alpha) \iota_k^\lambda (1 + \log(\lambda)) \omega}{C p \lambda \eta} \right).$$

Where

$$(3.6) \quad \iota_{k+1}^\lambda(\alpha) = \sum_{i=k-\lambda+1}^k \frac{\|S'_{i+1} r_i\|_2^4}{\lambda} = \sum_{i=k-\lambda+1}^k \frac{\|\tilde{r}_i\|_2^4}{\lambda},$$

which requires an additional  $\mathcal{O}(\lambda)$  operations after computing (3.4). The credible interval is established in [Corollary 4.8](#), and the consistency of the estimated credible interval follows from [Theorem 4.6](#). By virtue of being based on a high-probability bound, the credible interval tends to conservatively estimate the appropriate width of the  $(1 - \alpha)$ -credible interval, which warrants a contraction parameter,  $\eta \geq 1$ , to allow for numerical-evidence driven adjustments to the width. Conservative values of the contraction parameter,  $\eta$ , are presented in [Table 3](#).

Table 3: Conservative choices of the contraction parameter,  $\eta$ , by sketching method based on the experiments in [Appendix A.5](#).

Sampling Method	$\eta$
Gaussian [3]	13
Achlioptas [1]	13
FJLT [2]	188

*Stopping Condition.* As argued above, we want to stop the algorithm when the actual moving average of the residuals is less than a user-specified threshold  $v$ . In reality, we only have the estimated moving average of the residuals, (3.4), and we could instead consider stopping when  $\rho_k^\lambda \leq v$ . However, we may expect a possible discrepancy between the behavior of the estimated moving average and the actual moving average of the residuals. Therefore, informally, we propose a stopping condition that attempts to control this discrepancy in two ways:

1. it controls the probability that the estimate exceeds the threshold, while the actual moving average is less than the threshold by a user-specified factor of  $\delta_I \in (0, 1)$ —at a user-specified probability of  $\xi_I \in (0, 1)$ ; and

2. it controls the probability that the estimate is less than the threshold and the actual value exceeds the threshold by a factor of  $\delta_{II} > 1$ —at a user-specified probability of  $\xi_{II} \in (0, 1)$ .

Formally, these probabilities are controlled under the following situations (see [Corollary 4.9](#)). For the first mode of failure,

$$(3.7) \quad \begin{aligned} & (\|AB^{-1/2}\|_2 \|x_{k-\lambda+1} - x^*\|_B)^4 \leq \frac{Cp\lambda \min\{(1-\delta_I)^2 v^2, (1-\delta_I)v/\omega\}}{(1+\log(\lambda)) \log(2/\xi_I)} \Rightarrow \\ & \mathbb{P} \left[ \rho_{k+1}^\lambda > v, \sum_{i=k-\lambda+1}^k \frac{\|r_i\|_2^2}{\lambda} \leq \delta_I v \middle| \mathcal{F}_{k-\lambda+1} \right] < \xi_I, \end{aligned}$$

and, for the second mode of failure,

$$(3.8) \quad \begin{aligned} & (\|AB^{-1/2}\|_2 \|x_{k-\lambda+1} - x^*\|_B)^4 \leq \frac{Cp\lambda \min\{(\delta_{II}-1)^2 v^2, (\delta_{II}-1)v/\omega\}}{(1+\log(\lambda)) \log(2/\xi_{II})} \Rightarrow \\ & \mathbb{P} \left[ \rho_{k+1}^\lambda \leq v, \sum_{i=k-\lambda+1}^k \frac{\|r_i\|_2^2}{\lambda} > \delta_{II} v \middle| \mathcal{F}_{k-\lambda+1} \right] < \xi_{II}. \end{aligned}$$

Of course, these conditions can only be operationalized if  $\|AB^{-1/2}\|_2 \|x_{k-\lambda+1} - x^*\|_B$  in (3.7) and (3.8) is available, which it is not. Thus, these conditions can be made practical by replacing this unknown quantity with a corresponding lower-bound estimator,  $\iota_k^\lambda$  (see (3.6)), as justified in [Lemma 4.10](#). While using the lower bound estimate would produce an optimistic result, it turns out that the combination of the conservative tail-bound and use of  $\iota_k^\lambda$  balance well in practice, as shown in [section 5](#).

In summary, we stop the iterates when

$$(3.9) \quad \left\{ \begin{array}{l} \rho_k^\lambda \leq v \\ \iota_k^\lambda \leq \min \left\{ \frac{Cp\lambda\eta \min\{(1-\delta_I)^2 v^2, (1-\delta_I)v/\omega\}}{(1+\log(\lambda)) \log(2/\xi_I)}, \right. \\ \left. \frac{Cp\lambda\eta \min\{(\delta_{II}-1)^2 v^2, (\delta_{II}-1)v/\omega\}}{(1+\log(\lambda)) \log(2/\xi_{II})} \right\} \end{array} \right\} \quad \text{and}$$

are satisfied, where we have included the contraction parameter  $\eta$  to increase the upper bound threshold on  $\iota_k^\lambda$  owing to the conservativeness of the bounds.

**3.2. Tracking and Stopping with an Adaptive Moving Window.** As shown in [Figure 1a](#), IRS methods commonly have two phases of behavior: an initial “convergence” phase in which changes to the residual norm are dominated by a

rapid convergence to the solution, and a subsequent “noisy” phase in which changes to the residual norm are dominated by the algorithm’s noise. Thus, as shown in [Figure 1a](#), tracking an IRS method with a fixed moving average will lag (depending on the window width) during the initial phase before catching up during the subsequent phase. To ameliorate this issue, we propose to use multiple widths: a small  $\lambda_1 \in \mathbb{N}$  for the convergence phase; a  $\lambda_2 > \lambda_1$  for the noisy phase; and an intermediate phase that increments by one from  $\lambda_1$  to  $\lambda_2$  once the change in phases occurs. However, we need a method to detect the iterate,  $k'$ , at which the transition from one phase to another occurs.

A naive yet effective choice is to let  $k'$  be the first iterate  $k$  at which

$$(3.10) \quad \|\tilde{r}_k\|_2 = \|S'_{k+1}r_k\|_2 \geq \|S'_k r_{k-1}\|_2 = \|\tilde{r}_{k-1}\|_2,$$

and to let the moving average window be

$$(3.11) \quad \lambda = \begin{cases} \lambda_1 & k \leq k' \\ \lambda_1 + 1 + (k - k') & k \in [k', k' + (\lambda_2 - \lambda_1 - 1)] \\ \lambda_2 & k \geq k' + (\lambda_2 - \lambda_1 - 1). \end{cases}$$

That is,  $k'$  is the first time that the sketched residual norm increases.

With this choice of  $k'$  there are two cases that can happen. In the first case,  $k'$  is triggered in some finite time. In this case, the moving average window transitions from  $\lambda_1$  to  $\lambda_2$  as we want. In the second case,  $k'$  is never triggered. In this case, the moving average window remains  $\lambda_1$  and  $\|S'_{k+1}r_k\|_2$  decays monotonically, which is indicative of the residuals converging to zero owing to [Definition 3.3](#) (see [Theorem 4.6](#)). Therefore, in either case, this choice of  $k'$  leads to a desirable outcome.

**4. Consistency of Estimators and Intervals.** To demonstrate the theoretical soundness of our algorithms, we need to demonstrate the validity of the estimated residual-norm moving average ( $\rho_k^\lambda$ ), the estimated credible interval, and the estimated stopping criterion (see [\(3.4\)](#), [\(3.5\)](#), and [\(3.9\)](#), respectively). In [subsection 4.2](#), the consistency of the estimated residual-norm moving average is established in [Theorem 4.6](#), and then we show that the distribution of the estimated residual-norm moving average is sub-Exponential (see [Theorem 4.7](#)), which relies on the results established in [subsection 4.1](#). Using this latter fact about the estimated residual-norm moving average, we derive the estimator’s actual credible interval (see [\(4.32\)](#)) and validate the actual stopping criterion (see [Corollary 4.9](#)). Subsequently, in [subsection 4.3](#), we justify using  $\iota_k^\lambda$  as a plug-in estimator for the unknowns in the actual credible interval and stopping criterion (see [Lemma 4.10](#)).

**4.1. Convergence of the Residuals’ Moments.** Our goal is to prove that all the moments of the residual will converge to zero. To achieve this goal, we will show that the moments of the absolute error converge to zero. To this end, we will transform the iteration update, [\(3.2\)](#), into a more amenable form. As we will see, this more amenable form shows that the updates are a sequence of orthogonal projections. Using these orthogonal projections and [\[9, Theorem 4.1\]](#), we will show that, at a random iteration, a sufficient, random geometric reduction in the error will occur. Our final step will be to control the random iteration and the random reduction in the error. Once these pieces are in place, we will be able to conclude that the moments of the absolute error and, hence, the residual, decay (geometrically) to zero.



**Algorithm 3.2** Tracking and Stopping with a Adaptive Moving Window

---

**Require:**  $A \in \mathbb{R}^{m \times n}$ ,  $b \in \mathbb{R}^m$ ,  $x_0 \in \mathbb{R}^n$   
**Require:**  $\alpha, \xi_I, \xi_{II}, \delta_I \in (0, 1)$ ,  $\delta_{II} > 1$ ,  $\eta \geq 1$ ,  $v$   
**Require:** Random sketching method satisfying [Definition 3.3](#)  
**Require:** Moving window size  $\lambda_1 \leq \lambda_2 \in \mathbb{N}$

$k \leftarrow 0$   
 $k' \leftarrow \infty$   
 $\rho_0^* \leftarrow 0$   
 $\iota_0^* \leftarrow 0$

**while**  $k == 0$  **or** (3.9) fails to hold **do**  
  # Iteration  $k$  #  
  Generate  $(\tilde{A}, \tilde{b})$  from randomly sketch,  $S_{k+1}$ , and the original system,  $(A, b)$ .  
   $\tilde{r}_k = \tilde{A}x_k - \tilde{b}$   
  **if**  $\tilde{r}_k \geq \tilde{r}_{k-1}$  **then**  
     $k' \leftarrow k$   
  **end if**  
  Compute  $\lambda$  according to (3.11).  
  Update moving average  $\rho_k^\lambda$  from  $\rho_{k-1}^\lambda$ ; see (3.4).  
  Update fourth moment estimate  $\iota_k^\lambda$  from  $\iota_{k-1}^\lambda$ ; see (3.6).  
  Update the estimated  $(1 - \alpha)$ -interval; see (3.5).  
  Update iterate  $x_{k+1}$  from  $x_k$ ; see (3.2).  
   $k \leftarrow k + 1$   
**end while**  
**return**  $x_k$  **and** estimated  $(1 - \alpha)$ -interval

---

*Transformation of Variables.* To avoid unnecessary considerations about inner products, we will begin by a transformation of the variables by a symmetric square root of  $B$ . In other words, (3.2) becomes

$$(4.1) \quad B^{1/2}x_{k+1} = B^{1/2}x_k - B^{-1/2}A'S_{k+1}(S'_{k+1}AB^{-1}A'S_{k+1})^\dagger S'_{k+1}(Ax_k - b).$$

Furthermore, by letting  $x^*$  be the projection of  $x_0$  onto the solution set of (3.1) under [Assumption 3.1](#) and letting  $\beta_k = B^{1/2}(x_k - x^*)$ ,

$$(4.2) \quad \beta_{k+1} = \beta_k - B^{-1/2}A'S_{k+1}(S'_{k+1}AB^{-1}A'S_{k+1})^\dagger S'_{k+1}AB^{-1/2}\beta_k.$$

From (4.2), we observe that  $B^{-1/2}A'S_{k+1}(S'_{k+1}AB^{-1}A'S_{k+1})^\dagger S'_{k+1}AB^{-1/2}$  is an orthogonal projection onto  $\text{row}(S'_{k+1}AB^{-1/2})$ . As a result, we have an observation and a useful simplification. First, we observe that the projection of  $\beta_k$  onto the kernel of  $AB^{-1/2}$  is zero for all  $k$  owing to the (4.2) and the definition of  $x^*$ ; that is,  $\beta_k$  are all in  $\text{row}(AB^{-1/2})$ . Second, if we let  $Q_{k+1}$  be a matrix with orthonormal columns that form a basis for  $\text{row}(S'_{k+1}AB^{-1/2})$ , then (4.2) becomes

$$(4.3) \quad \beta_{k+1} = \beta_k - Q_{k+1}Q'_{k+1}\beta_k.$$

*Geometric Reduction in Error.* Now, let  $\tau_0 = 0$  and let  $\tau_1$  be the first iteration such that

$$(4.4) \quad \text{col}(Q_1) + \text{col}(Q_2) + \cdots + \text{col}(Q_{\tau_1}) = \text{row}(AB^{-1/2}),$$

otherwise let  $\tau_1$  be infinite. When  $\tau_1$  is finite, we have the following result.

LEMMA 4.1. *Let  $x_0 \in \mathbb{R}^n$  and  $x^*$  be its projection onto the solution set of (3.1) under Assumption 3.1. Let  $\{x_k\}$  be generated according to (3.2) for arbitrary  $\{S_k\}$ . On the event,  $\{\tau_1 < \infty\}$ , there exists a  $\gamma_1 \in (0, 1)$  that is a function of  $\{Q_1, \dots, Q_{\tau_1}\}$  such that*

$$(4.5) \quad \|x_{\tau_1} - x^*\|_B \leq \gamma_1 \|x_0 - x^*\|_B.$$

*Proof.* By our definition of  $\beta_k$ , we need only prove that  $\exists \gamma_1 \in (0, 1)$  such that  $\|\beta_{\tau_1}\|_2 \leq \gamma_1 \|\beta_0\|_2$ . To prove this, let  $q_{k,1}, \dots, q_{k,p}$  denote the columns of  $Q_k$ . Then, by (4.3),

$$(4.6) \quad \beta_{\tau_1} = \left[ \prod_{k=1}^{\tau_1} \left( \prod_{j=1}^p (I - q_{k,j} q'_{k,j}) \right) \right] \beta_0$$

Since  $\beta_0 \in \text{row}(AB^{-1/2})$ , [9, Theorem 4.1] implies that there exists a  $\gamma_1 \in (0, 1)$  that is a function of  $\{q_{1,1}, q_{1,2}, \dots, q_{\tau_1,p-1}, q_{\tau_1,p}\}$  such that  $\|\beta_{\tau_1}\|_2 \leq \gamma_1 \|\beta_0\|_2$ .  $\square$

We need not stop at  $\tau_1$ . In fact, we can iterate on this argument in the following manner. When  $\{\tau_\ell < \infty\}$ , define  $\tau_{\ell+1}$  to be the first iteration after  $\tau_\ell$  such that

$$(4.7) \quad \text{col}(Q_{\tau_{\ell+1}}) + \text{col}(Q_{\tau_{\ell+2}}) + \dots + \text{col}(Q_{\tau_{\ell+1}}) = \text{row}(AB^{-1/2}),$$

otherwise let  $\tau_{\ell+1}$  be infinite. Then, we have the following straightforward corollary.

COROLLARY 4.2. *Let  $x_0 \in \mathbb{R}^n$  and  $x^*$  be its projection onto the solution set of (3.1) under Assumption 3.1. Let  $\{x_k\}$  be generated according to (3.2) for arbitrary  $\{S_k\}$ . On the event,  $\cap_{\ell=1}^L \{\tau_\ell < \infty\}$ , there exists  $\gamma_\ell \in (0, 1)$  that is a function of  $\{Q_{\tau_{\ell-1}+1}, \dots, Q_{\tau_\ell}\}$  for  $\ell = 1, \dots, L$ , such that*

$$(4.8) \quad \|x_{\tau_L} - x^*\|_B \leq \left( \prod_{\ell=1}^L \gamma_\ell \right) \|x_0 - x^*\|_B.$$

*Control of the Random Rate and Random Iteration.* Of course, Corollary 4.2 does not imply that the absolute error converges to zero. In fact, Corollary 4.2 has two points of failure. First, it may happen that  $\gamma_\ell \rightarrow 1$  as  $\ell \rightarrow \infty$  with some nonzero probability; that is, we have no control over the random rate of convergence. This issue is addressed by the following result, which relies on the independence of  $\{S_k\}$ .

LEMMA 4.3. *Let  $\{S_k : k \in \mathbb{N}\}$  be independent and identically distributed random variables. Then, whenever they are well-defined,  $\{\tau_\ell - \tau_{\ell-1} : \ell \in \mathbb{N}\}$  are independent and identically distributed; and  $\{\gamma_\ell : \ell \in \mathbb{N}\}$  are independent and identically distributed.*

*Proof.* When  $\tau_\ell$  is finite, by [4, Theorem 4.1.3],  $\{Q_{\tau_{\ell+1}}, \dots, Q_{\tau_{\ell+k}}\}$  given  $\tau_\ell$  are independent of  $\{Q_1, \dots, Q_{\tau_\ell}\}$  and are identically distributed to  $\{Q_1, \dots, Q_k\}$  for all  $k$ . Therefore,  $\tau_\ell - \tau_{\ell-1}$  are independent and identically distributed, as are  $\gamma_\ell$ .  $\square$

The second point of failure in Corollary 4.2, as alluded to in Lemma 4.3, is the existence of  $\{\tau_\ell\}$ . Specifically, on  $\{\tau_\ell = \infty\}$ , Corollary 4.2 will no longer supply a rate of improvement in the absolute error. Therefore, we must show that  $\{\tau_\ell < \infty\}$  occurs with probability one, which is the content of the next result.

LEMMA 4.4. *Let  $\{S_k : k \in \mathbb{N}\}$  be independent and identically distributed random variables satisfying Definition 3.3. If*

$$(4.9) \quad p > \frac{\log(2)}{C} \max \left\{ \omega^2, \frac{1}{\delta^2} \right\},$$

for some  $\delta \in (0, 1)$ , then  $\mathbb{P}(\tau_\ell < \infty) = 1$  for every  $\ell \in \mathbb{N}$  and  $\exists \pi \in (0, 1]$  such that, for all  $\ell \in \mathbb{N}$  and  $k \geq \text{rank}(A)$ ,

$$(4.10) \quad \mathbb{P}(\tau_\ell - \tau_{\ell-1} = k) \leq \binom{k-1}{\text{rank}(A)-1} (1-\pi)^{k-\text{rank}(A)} \pi^{\text{rank}(A)}.$$

*Proof.* We begin by verifying that if  $z \in \text{row}(AB^{-1/2})$  then  $S'_1 AB^{-1/2} z \neq 0$  with some nonzero probability. Definition 3.3 implies, for any  $\delta \in (0, 1)$ ,

$$(4.11) \quad \mathbb{P} \left( \|S'_1 AB^{-1/2} z\|_2^2 > 0 \right) \geq \mathbb{P} \left( \left| \|S'_1 AB^{-1/2} z\|_2^2 - \|AB^{-1/2} z\|_2^2 \right| \leq \delta \|AB^{-1/2} z\|_2^2 \right)$$

$$(4.12) \quad \geq 1 - 2e^{-\min\{Cp\delta^2, (Cp\delta)/\omega\}}.$$

When we choose  $\delta \in (0, 1)$  such that (4.9) holds, then  $1 - 2e^{-\min\{Cp\delta^2, Cp\delta\}} > 0$ . Moreover, as this bound is independent of  $z \in \text{row}(AB^{-1/2})$ , we refer to the lower bound of  $\mathbb{P}(\|S'_1 AB^{-1/2} z\|_2^2 > 0)$  for any  $z \in \text{row}(AB^{-1/2})$  by  $\pi \in (0, 1]$ . To summarize, given the relationship between  $Q_1$  and  $\text{row}(S'_1 AB^{-1/2})$ ,  $\mathbb{P}(\|Q'_1 z\|_2 > 0) \geq \pi$  for all  $z \in \text{row}(AB^{-1/2})$ .

Given that  $\{Q_k : k \in \mathbb{N}\}$  are independent and identically distributed, we conclude that the probability that  $\text{col}(Q_1) + \dots + \text{col}(Q_{k+1})$  grows in dimension relative to  $\text{col}(Q_1) + \dots + \text{col}(Q_k)$ , when  $\dim(\text{col}(Q_1) + \dots + \text{col}(Q_k)) < \text{rank}(A)$ , is at least  $\pi$ . As a result, the probability that the dimension increases  $\text{rank}(A)$  times in the first  $k$  iterations with  $k \geq \text{rank}(A)$  is dominated by a negative binomial distribution. In other words, for  $k \geq \text{rank}(A)$ ,

$$(4.13) \quad \mathbb{P}(\tau_1 = k) \leq \binom{k-1}{\text{rank}(A)-1} (1-\pi)^{k-\text{rank}(A)} \pi^{\text{rank}(A)}.$$

Therefore,  $\tau_1$  is finite with probability one. The result follows by Lemma 4.3.  $\square$

*Convergence of the Moments.* We now put these pieces together to conclude as follows.

THEOREM 4.5. *Let  $x_0 \in \mathbb{R}^n$  and  $x^*$  be its projection onto the solution set of (3.1) under Assumption 3.1. Suppose  $\{S_k : k \in \mathbb{N}\}$  are independent and identically distributed random variables satisfying Definition 3.3 and (4.9) for some  $\delta \in (0, 1)$ . Finally, let  $\{x_k\}$  be generated according to (3.2). Then, for any  $d \in \mathbb{N}$ ,  $\mathbb{E}[\|Ax_k - b\|_2^d] \rightarrow 0$  and  $\mathbb{E}[\|x_k - x^*\|_B^d] \rightarrow 0$  as  $k \rightarrow \infty$ . Additionally, for any particular  $\ell$  we have*

$$(4.14) \quad \mathbb{E}[\|x_{\tau_\ell} - x^*\|_B^d] \leq \mathbb{E}[\gamma_1^d]^\ell \|x_0 - x^*\|_B^d.$$

*Proof.* It is enough to show that  $\mathbb{E}[\|x_k - x^*\|_B^d] \rightarrow 0$  as  $k \rightarrow \infty$ . By (4.3), the absolute error is a non-increasing sequence. Thus, we need only show that a subsequence converges to zero. By Corollary 4.2 and Lemmas 4.3 and 4.4,

$$(4.15) \quad \mathbb{E}[\|x_{\tau_\ell} - x^*\|_B^d] \leq \mathbb{E}[\gamma_1^d]^\ell \|x_0 - x^*\|_B^d,$$

for all  $\ell \in \mathbb{N}$ , where  $\mathbb{E}[\gamma_1^d] < 1$ . Therefore, as  $\ell \rightarrow \infty$ , the conclusion follows.  $\square$

**4.2. Properties of the Point Estimators.** Using [Theorem 4.5](#), we first show that  $\rho_k^\lambda$  and  $\iota_k^\lambda$  are consistent estimators for  $\lambda^{-1} \sum_{i=k-\lambda+1}^k \|r_k\|_2^d$  for  $d \in \{2, 4\}$ , respectively. Then, we derive a tail distribution for  $\rho_k^\lambda$ , from which we can derive a credible interval and a stopping criterion. Unfortunately, these latter two quantities will involve unknown quantities about the distribution of  $\rho_k^\lambda$  and will need to be estimated, which is the subject of the next subsection.

**THEOREM 4.6.** *Suppose the setting of [Theorem 4.5](#) holds. Then, for  $d \in \{2, 4\}$ ,*

$$(4.16) \quad \lim_{k \rightarrow \infty} \mathbb{P} \left( \left| \sum_{i=k-\lambda+1}^k \frac{\|\tilde{r}_i\|_2^d}{\lambda} - \sum_{i=k-\lambda+1}^k \frac{\|r_i\|_2^d}{\lambda} \right| > \epsilon \right) = 0,$$

where  $\tilde{r}_i = S'_{i+1} r_i$ .

*Proof.* Using the triangle inequality and the union bound,

$$(4.17) \quad \mathbb{P} \left( \left| \sum_{i=k-\lambda+1}^k \frac{\|\tilde{r}_i\|_2^d - \|r_i\|_2^d}{\lambda} \right| > \epsilon \right) \leq \mathbb{P} \left( \bigcup_{i=k-\lambda+1}^k \left\{ \left| \frac{\|\tilde{r}_i\|_2^d - \|r_i\|_2^d}{\lambda} \right| > \frac{\epsilon}{\lambda} \right\} \right)$$

$$(4.18) \quad \leq \sum_{i=k-\lambda+1}^k \mathbb{P} \left( \left| \frac{\|\tilde{r}_i\|_2^d - \|r_i\|_2^d}{\lambda} \right| > \frac{\epsilon}{\lambda} \right).$$

Now, by Markov's inequality and the independence of  $\{S_k\}$ ,

$$(4.19) \quad \sum_{i=k-\lambda+1}^k \mathbb{P} \left( \left| \frac{\|\tilde{r}_i\|_2^d - \|r_i\|_2^d}{\lambda} \right| > \frac{\epsilon}{\lambda} \right) \leq \sum_{i=k-\lambda+1}^k \frac{\mathbb{E}[\|\tilde{r}_i\|_2^d + \|r_i\|_2^d]}{\epsilon}$$

$$(4.20) \quad \leq \sum_{i=k-\lambda+1}^k \frac{\mathbb{E}[\|S_{i+1}\|_2^d \|r_i\|_2^d + \|r_i\|_2^d]}{\epsilon}$$

$$(4.21) \quad \leq \sum_{i=k-\lambda+1}^k \frac{(\mathbb{E}[\|S_{i+1}\|_2^d] + 1) \mathbb{E}[\|r_i\|_2^d]}{\epsilon}.$$

By [Lemma A.3](#),  $\mathbb{E}[\|S_{k+1}\|_2^2]$  and  $\mathbb{E}[\|S_{k+1}\|_2^4]$  are bounded by their own respective constants meaning [Theorem 4.5](#) implies the result as  $k \rightarrow \infty$ .  $\square$

With consistency established, we now turn to understanding  $\rho_k^\lambda$ 's distribution. Intuitively, as the terms in the definition of  $\rho_k^\lambda$  satisfy the [Definition 3.3](#), we would trivially have that  $\rho_k^\lambda$  satisfies [Definition 3.3](#) if its terms are independent. Unfortunately, the terms in the definition of  $\rho_k^\lambda$  are not independent, yet we can prove that this estimator still satisfies [Definition 3.3](#) with an additional logarithmic term relative to the case in which the terms had been independent.

**THEOREM 4.7.** *Suppose the setting of [Theorem 4.5](#) holds. Define  $\mathcal{F}_{k-\lambda+1}$  be the minimal  $\sigma$ -algebra around  $S_1, \dots, S_{k-\lambda+1}$ , then*

$$(4.22) \quad \rho_k^\lambda \Big|_{\mathcal{F}_{k-\lambda+1}} \sim \mathbf{SE} \left( \frac{M_{k-\lambda+1}^4 (1 + \log(\lambda))}{2Cp\lambda}, \omega \right).$$

Where  $M_{k-\lambda+1} = \|AB^{-1/2}\|_2 \|x_{k-\lambda+1} - x^*\|_B$ .

*Proof.* By induction, we prove, for  $|t| \leq 1/\omega$ ,

$$(4.23) \quad \mathbb{E} \left[ \prod_{i=k-\lambda+1}^k \exp \left\{ \frac{t}{\lambda} (\|\tilde{r}_i\|_2^2 - \|r_i\|_2^2) \right\} \middle| \mathcal{F}_{k-\lambda+1} \right] \leq \exp \left( \frac{t^2 M_{k-\lambda+1}^4}{2Cp\lambda} \sum_{j=1}^{\lambda} \frac{1}{j} \right),$$

where  $M_{k-\lambda+1} = \|AB^{-1/2}\|_2 \|x_{k-\lambda+1} - x^*\|_B$ . We can then use a logarithm to bound the summation. As a result, the sub-exponential distribution of  $\rho_k^\lambda$  by [Lemma A.4](#).

The base case of  $\lambda = 1$  follows trivially from  $\|\tilde{r}_i\|_2^2$  being sub-Exponential. Now assume that the result holds up to  $\lambda - 1$ . Then,

$$(4.24) \quad \mathbb{E} \left[ \prod_{i=k-\lambda+1}^k \exp \left\{ \frac{t}{\lambda} (\|\tilde{r}_i\|_2^2 - \|r_i\|_2^2) \right\} \middle| \mathcal{F}_{k-\lambda+1} \right]$$

$$(4.25) \quad = \mathbb{E} \left[ \mathbb{E} \left[ \prod_{i=k-\lambda+1}^k \exp \left\{ \frac{t}{\lambda} (\|\tilde{r}_i\|_2^2 - \|r_i\|_2^2) \right\} \middle| \mathcal{F}_k \right] \middle| \mathcal{F}_{k-\lambda+1} \right]$$

$$= \mathbb{E} \left[ \mathbb{E} \left[ \exp \left\{ \frac{t}{\lambda} (\|\tilde{r}_k\|_2^2 - \|r_k\|_2^2) \right\} \middle| \mathcal{F}_k \right] \right]$$

$$(4.26) \quad \times \prod_{i=k-\lambda+1}^{k-1} \exp \left\{ \frac{t}{\lambda} (\|\tilde{r}_i\|_2^2 - \|r_i\|_2^2) \right\} \middle| \mathcal{F}_{k-\lambda+1} \right]$$

$$(4.27) \quad \leq \mathbb{E} \left[ \exp \left\{ \frac{t^2 \|r_k\|_2^4}{2\lambda^2 Cp} \right\} \prod_{i=k-\lambda+1}^{k-1} \exp \left\{ \frac{t}{\lambda} (\|\tilde{r}_i\|_2^2 - \|r_i\|_2^2) \right\} \middle| \mathcal{F}_{k-\lambda+1} \right],$$

where we have made use of  $\|\tilde{r}_k\|_2^2$  being sub-Exponential in the ultimate line. Now, applying Hölder's inequality and the induction hypothesis,

$$(4.28) \quad \mathbb{E} \left[ \exp \left\{ \frac{t^2 \|r_k\|_2^4}{2\lambda^2 Cp} \right\} \prod_{i=k-\lambda+1}^{k-1} \exp \left\{ \frac{t}{\lambda} (\|\tilde{r}_i\|_2^2 - \|r_i\|_2^2) \right\} \middle| \mathcal{F}_{k-\lambda+1} \right]$$

$$\leq \mathbb{E} \left[ \exp \left\{ \frac{t^2 \|r_k\|_2^4}{2\lambda Cp} \right\} \middle| \mathcal{F}_{k-\lambda+1} \right]^{\frac{1}{\lambda}}$$

$$(4.29) \quad \times \mathbb{E} \left[ \prod_{i=k-\lambda+1}^{k-1} \exp \left\{ \frac{t}{\lambda-1} (\|\tilde{r}_i\|_2^2 - \|r_i\|_2^2) \right\} \middle| \mathcal{F}_{k-\lambda+1} \right]^{\frac{\lambda-1}{\lambda}}$$

$$(4.30) \quad \leq \mathbb{E} \left[ \exp \left\{ \frac{t^2 \|r_k\|_2^4}{2\lambda Cp} \right\} \middle| \mathcal{F}_{k-\lambda+1} \right]^{\frac{1}{\lambda}} \exp \left\{ \frac{t^2 M_{k-\lambda+1}^4}{2Cp(\lambda-1)} \sum_{j=1}^{\lambda-1} \frac{1}{j} \right\}^{\frac{\lambda-1}{\lambda}}.$$

Now, [Corollary 4.2](#) and [Lemma 4.4](#) imply, with probability one,

$$(4.31) \quad \|r_k\|_2^4 \leq \|AB^{-1/2}\|_2^4 \|x_i - x^*\|_B^4 \leq \|AB^{-1/2}\|_2^4 \|x_{k-\lambda+1} - x^*\|_B^4 = M_{k-\lambda+1}^4.$$

Since  $M_{k-\lambda+1}$  is measurable with respect to  $\mathcal{F}_{k-\lambda+1}$ , we apply the previous inequality to [\(4.30\)](#) to conclude the proof by induction.  $\square$

With the establishment of the distribution around the difference between  $\rho_k^\lambda$  and the true moving average, we are now able to derive the credible interval and [\(3.9\)](#).

COROLLARY 4.8. *A credible interval of level  $1 - \alpha$  for the procedure defined in (3.4) is*

$$(4.32) \quad \rho_k^\lambda \pm \max \left( \sqrt{2 \log(2/\alpha) \frac{M_{k-\lambda+1}^4 (1 + \log(\lambda))}{Cp\lambda}}, \right. \\ \left. 2 \log(2/\alpha) \frac{M_{k-\lambda+1}^4 (1 + \log(\lambda)) \omega}{Cp\lambda} \right).$$

*Proof.* Using the sub-Exponential variance from Theorem 4.7, the tail bound result from Proposition 2.9 of [12],

$$(4.33) \quad \mathbb{P} \left( \left| \rho_k^\lambda - \sum_{i=k-\lambda+1}^k \frac{\|r_i\|_2^2}{\lambda} \right| > \epsilon \right) \leq 2 \exp \left( - \frac{Cp\lambda}{2M_{k-\lambda+1}^4 (1 + \log(\lambda))} \min \left( \epsilon^2, \frac{\epsilon}{\omega} \right) \right).$$

From this tail probability it should be clear that the high probability region is controlled by the choice of  $\epsilon$  thus if we choose  $\epsilon$  such that it lines up with a specific quantile  $\alpha$  we will have our desired confidence region.

$$(4.34) \quad \alpha = 2 \exp \left( - \frac{Cp\lambda}{2M_{k-\lambda+1}^4 (1 + \log(\lambda))} \min \left( \epsilon^2, \frac{\epsilon}{\omega} \right) \right).$$

Solving for  $\epsilon$  supplies  $\epsilon$  to be

$$(4.35) \quad \max \left( \sqrt{2 \log(2/\alpha) \frac{M_{k-\lambda+1}^4 (1 + \log(\lambda))}{Cp\lambda}}, 2 \log(2/\alpha) \frac{M_{k-\lambda+1}^4 (1 + \log(\lambda)) \omega}{Cp\lambda} \right). \quad \square$$

We finish this section by describing the methodology by which to derive the error control condition for the stopping criterion. The process will be the same for both types of errors thus we will show the work only for the 1st error type.

COROLLARY 4.9. *Given  $v$ ,  $\delta_I$ ,  $\xi_I$ ,  $\delta_{II}$ ,  $\xi_{II}$  as defined in subsection 3.1 and a sampling matrix satisfying Definition 3.3, then (3.7) and (3.8) are true.*

*Proof.* First,

$$(4.36) \quad \mathbb{P} \left( \rho_k^\lambda > v, \sum_{i=k-\lambda+1}^k \frac{\|r_i\|_2^2}{\lambda} \leq \delta_I v \middle| \mathcal{F}_{k-\lambda+1} \right) \\ \leq \mathbb{P} \left( \rho_k^\lambda - \sum_{i=k-\lambda+1}^k \frac{\|r_i\|_2^2}{\lambda} > v(1 - \delta_I), \sum_{i=k-\lambda+1}^k \frac{\|r_i\|_2^2}{\lambda} \leq \delta_I v \middle| \mathcal{F}_{k-\lambda+1} \right)$$

$$(4.37) \quad \leq \mathbb{P} \left( \rho_k^\lambda - \sum_{i=k-\lambda+1}^k \frac{\|r_i\|_2^2}{\lambda} > v(1 - \delta_I) \middle| \mathcal{F}_{k-\lambda+1} \right)$$

Using the sub-Exponential variance from Theorem 4.7 and the tail bound result from Proposition 2.9 of [12],

$$(4.38) \quad \mathbb{P} \left( \rho_k^\lambda - \sum_{i=k-\lambda+1}^k \frac{\|r_i\|_2^2}{\lambda} > v(1 - \delta_I) \right) \leq \\ \exp \left( - \frac{Cp\lambda}{2M_{k-\lambda+1}^4 (1 + \log(\lambda))} \min \left( v^2(1 - \delta_I)^2, \frac{v(1 - \delta_I)}{\omega} \right) \right).$$

Thus, when  $M_{k-\lambda+1} = \|AB^{-1/2}\|_2 \|x_{k-\lambda+1} - x^*\|_B$  satisfies (3.7), the right-hand side of the preceding inequality is bounded by  $\xi_I$ . We can repeat this argument to show that (3.8) is true.  $\square$

**4.3. Estimating the Credible Interval and Stopping Criterion.** Corollaries 4.8 and 4.9 provide a well-controlled uncertainty set and stopping criterion, yet require knowing  $M_{k-\lambda+1}$ , which is usually not available. As stated before, Corollaries 4.8 and 4.9 can be operationalized by replacing  $M_{k-\lambda+1}^4$  with  $\iota_k^\lambda$ . Of course,  $M_{k-\lambda+1}^4$  and  $\iota_k^\lambda$  must coincide in some sense in order for this estimation to be valid. Indeed, by Theorems 4.5 and 4.6, both  $M_{k-\lambda+1}^4$  and  $\iota_k^\lambda$  converge to zero as  $k \rightarrow \infty$ , which would allow us to estimate  $M_{k-\lambda+1}^4$  with  $\iota_k^\lambda$  to generate consistent estimators. However, we could also estimate  $M_{k-\lambda+1}^4$  by 0 to generate consistent estimators, but these would be uninformative during finite time. Therefore, we must establish that estimating  $M_{k-\lambda+1}^4$  by  $\iota_k^\lambda$  is also appropriate within some finite time. In the next result, we establish that the relative error between  $M_{k-\lambda+1}^4$  and  $\iota_k^\lambda$  is controlled by a constant (in probability).

LEMMA 4.10. For  $M_{k-\lambda+1}^4$  as described in Theorem 4.7 and  $\iota_k^\lambda$  as defined in (3.6),

$$(4.39) \quad \mathbb{P} \left( \left| \frac{M_{k-\lambda+1}^4 - \iota_k^\lambda}{M_{k-\lambda+1}^4} \right| > 1 + \epsilon, M_{k-\lambda+1}^4 \neq 0 \right) \leq \frac{1 + \mathbb{E}[\|S_1\|_2^4]}{\epsilon},$$

where  $\mathbb{E}[\|S_1\|_2^4]$  is finite by Lemma A.3.

*Proof.* First,

$$(4.40) \quad \left| \frac{M_{k-\lambda+1}^4 - \iota_k^\lambda}{M_{k-\lambda+1}^4} \right| \leq \left| \frac{M_{k-\lambda+1}^4 - \sum_{i=k-\lambda+1}^k \frac{\|r_i\|_2^4}{\lambda}}{M_{k-\lambda+1}^4} \right| + \left| \frac{\sum_{i=k-\lambda+1}^k \frac{\|r_i\|_2^4}{\lambda} - \iota_k^\lambda}{M_{k-\lambda+1}^4} \right|,$$

Moreover,

$$(4.41) \quad \sum_{i=k-\lambda+1}^k \frac{\|r_i\|_2^4}{\lambda} \in \left[ \sigma_{\min}(AB^{-1/2})^4 \|x_k - x^*\|_B^4, M_{k-\lambda+1}^4 \right].$$

Applying this fact to (4.40),

$$(4.42) \quad \left| \frac{M_{k-\lambda+1}^4 - \iota_k^\lambda}{M_{k-\lambda+1}^4} \right| \leq 1 + \left| \frac{\sum_{i=k-\lambda+1}^k \frac{\|r_i\|_2^4}{\lambda} - \iota_k^\lambda}{M_{k-\lambda+1}^4} \right|.$$

We now apply Markov's inequality to the second term on the right-hand side, which supplies

$$(4.43) \quad \begin{aligned} & \mathbb{P} \left( \left| \frac{\sum_{i=k-\lambda+1}^k \frac{\|r_i\|_2^4}{\lambda} - \iota_k^\lambda}{M_{k-\lambda+1}^4} \right| > \epsilon \middle| \mathcal{F}_{k-\lambda+1} \right) \\ & \leq \frac{\sum_{i=k-\lambda+1}^k \mathbb{E} \left[ \|r_i\|_2^4 (1 + \|S_{i+1}\|_2^4) \middle| \mathcal{F}_{k-\lambda+1} \right]}{M_{k-\lambda+1}^4 \lambda \epsilon}. \end{aligned}$$

Since  $\|r_i\|_2^4 \leq M_{k-\lambda+1}^4$  with probability one for  $i \geq k - \lambda + 1$ , the result follows.  $\square$

Owing to [Lemma 4.10](#), the relative error between  $\iota_k^\lambda$  and  $M_{k-\lambda+1}$  is reasonably well controlled for practical purposes. As a result, we can use  $\iota_k^\lambda$  as a plug-in estimator for  $M_{k-\lambda+1}$  for the credible interval, [\(4.32\)](#), to produce the estimated credible interval suggested in [\(3.5\)](#); and we do the same for the stopping condition controls in [\(3.7\)](#) and [\(3.8\)](#) to produce the estimated stopping criterion in [\(3.9\)](#).

**5. Experimental results.** Using square consistent linear systems generated from coefficient matrices supplied by [\[13\]](#), we now numerically verify that our theory is valid, that our resulting estimators are useful, and that our algorithms actually scale and perform as expected to a realistically-sized problem. We organize these numerical experiments as follows.

1. In [subsection 5.1](#), we verify [Theorems 4.6](#) and [4.7](#)—that is,  $\rho_k^\lambda$  and  $\iota_k^\lambda$  are consistent estimators for  $\lambda^{-1} \sum_{i=k-\lambda+1}^k \|r_i\|_2^d$  for  $d \in \{2, 4\}$ , respectively.
2. In [subsection 5.2](#), we examine the performance of [\(3.5\)](#)—that is, we numerically test the estimated credible interval’s coverage probability.
3. In [subsection 5.3](#), we examine the performance of [\(3.9\)](#)—that is, we numerically test the estimated stopping criterion’s probability controls.
4. In [subsection 5.4](#), we run our algorithm on a system with a Rohess coefficient matrix of dimension  $16,384 \times 16,384$ , and show that our estimated credible interval captures the true residual of system and the stopping criterion appropriately stops the algorithm.

**5.1. Consistency of Estimators.** We simulate solving 44 square consistent linear systems of dimension 512 using iterative random sketching (IRS) for all three sketching schemes (i.e., Achlioptas, Gaussian, FLJT), and record the absolute differences between  $\rho_k^{100}$  and  $\iota_k^{100}$  and the quantities they are estimating. We present the results in [Figures 2](#) and [3](#), and panel the results along those situations according to whether the true residual moving average falls below  $10^{-8}$  within 1000 iterations. As we would expect from [Theorems 4.6](#) and [4.7](#), [Figures 2](#) and [3](#) show that the consistency of our estimators depends on the convergence of the underlying procedure: when the underlying procedure is converging, our estimators are guaranteed to perform well. Interestingly, [Figures 2](#) and [3](#) also show that, even when convergence is very slow (right panels), the estimators are quite accurate across at least 50% of the systems considered.

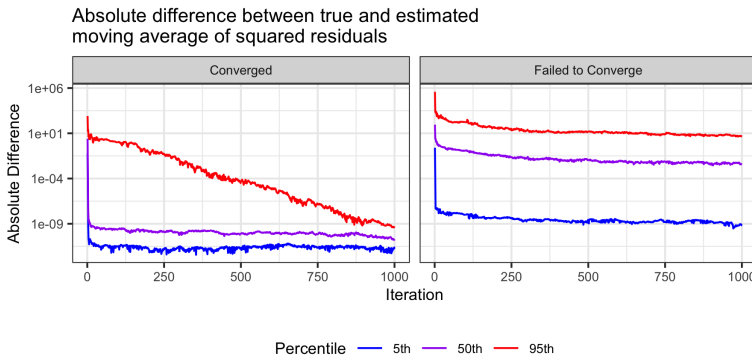


Fig. 2: Distribution of absolute errors of  $\rho_k^{100}$  under the converged and failed to converged scenarios.



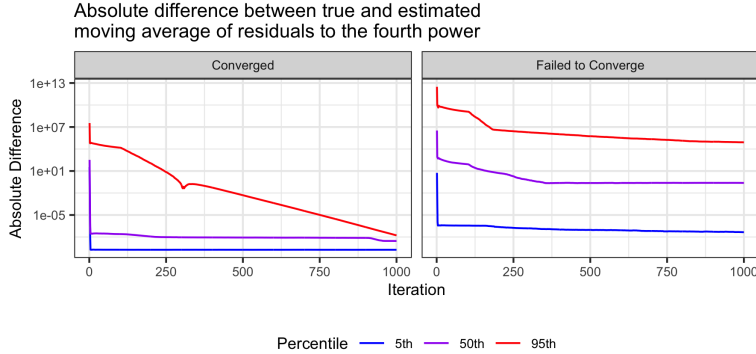


Fig. 3: Distribution of absolute errors of  $\iota_k^{100}$  under the converged and failed to converged scenarios.

**5.2. Estimated Credible Intervals.** We evaluate whether the estimated credible intervals, (3.5), actually have a coverage probability of  $1 - \alpha$  for  $\alpha = 0.05$ . To do so, we solve three distinct square systems of dimension 256 using IRS with the Gaussian sampling scheme with embedding dimension  $p = 25$ ; we compute the estimated credible interval at each iteration following (3.5) with a window of size 15; and we store all the iterates. Then, at each stored iterate, we independently simulate 1000 IRS solvers initialized at the iterate, and compute the actual residual moving average for each simulation. We then record these simulated residual moving averages at each iteration (i.e., 1000 at each iteration), and record number of times that the simulated residual moving averages exceed the estimated credible interval at each iterate. If our estimate of the credible interval is useful, then this proportion should not exceed  $\alpha = 0.05$ .

The estimated credible interval and simulated residuals for each iteration are plotted in Figure 4. Figure 4 shows that the credible interval contains all 1000 simulated residual moving averages at each iteration when  $\eta = 1$ , and is rarely exceeded when  $\eta$  is set to the values in Table 3. Thus, our estimated credible interval captures the uncertainty of the estimated residual moving average quite well, and the tightness of these intervals can be improved using the contraction parameter values in Table 3.

**5.3. Estimated Stopping Criterion.** We evaluate whether the satisfaction of the  $\iota_k^\lambda$  portion of the stopping condition, (3.9), fails to control the stopping errors (3.7) and (3.8) at rates of no more than  $\xi_I$  and  $\xi_{II}$  respectively. We use the same systems and sketching methods as in subsection 5.2, and we will use different values of  $v$  depending on how IRS performs on each system. The parameters  $(\delta_I, \delta_{II}, \xi_I, \xi_{II})$  are set to  $(0.9, 1.1, 0.01, 0.01)$ . We simulate IRS for each system and sketching method 1000 times for 500 iterations we then find the iterations where  $\iota_k^\lambda$  portion of the stopping condition, (3.9), is triggered, and determined whether (3.7), (3.8), or no error has occurred at each of those iterations. In Figure 5, the relative frequencies of each possible outcome when the  $\iota_k^\lambda$  condition of (3.9) for the Gaussian sketching method are plotted (the other methods are plotted in Figure 8). In Figure 5a, we let the contraction parameter be  $\eta = 1$ , while in Figure 5b, we let the contraction parameter be set to the values in Table 3. If the estimated stopping condition is appropriate, then we should expect no more than 20 incorrect observations per system. Indeed,

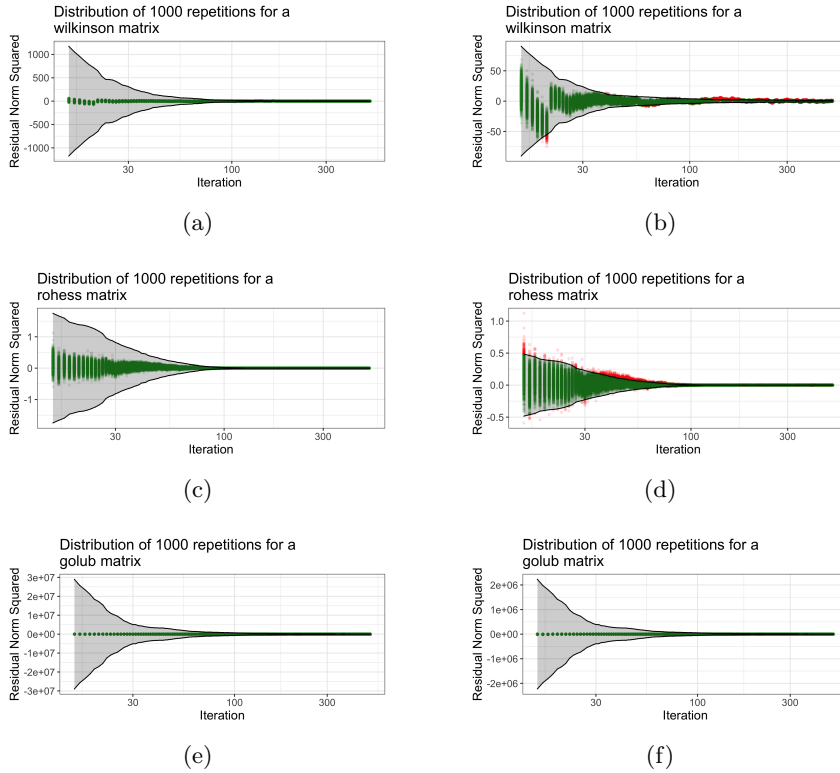


Fig. 4: The estimated 0.95-credible intervals (grey), their boundaries (black lines), simulated averaged residuals within the intervals (green), and simulated averaged residuals exceeding the interval (red). Plots (a) and (b) correspond to a Wilkinson coefficient matrix, (c) and (d) correspond to a Rohess coefficient matrix, and (e) and (f) correspond to a Golub coefficient matrix. Plots (a), (c) and (e) correspond to  $\eta = 1$ . Plots (b), (d), and (f) correspond to  $\eta$  in Table 3. The estimated credible interval is exceeded only in cases (b) and (d) by 2.4% of simulations on average (over iterations) and 9.1% of simulations on average (over iterations).

Figure 5 shows that the estimated stopping condition matches is appropriate, as there are 0 incorrect observations per system for  $\eta = 1$  and  $\eta$  set to the values in Table 3.

**5.4. Realistic System Example.** We now run Algorithm 3.2 to a square system of dimension  $16384 \times 16384$  with Rohess coefficient matrix, using an embedding dimension of  $p = 330$  and Gaussian sketching. The estimated residual moving average, estimated 0.95-credible interval and actual residual moving average are displayed in Figure 6. As Figure 6 shows, the estimated 0.95-credible interval with  $\eta = 13$  successfully covered 97.6% of the actual residual moving averages, which is above our desired 95% target. Moreover, the stopping condition with  $v = 1$  was triggered, and successfully stopped without making an error of the form (3.7), or (3.8).

**6. Conclusions.** To make iterative random sketching a more complete method, we have presented an estimator to track the moving average of the residual norms of



Fig. 5: Relative Frequency plots for 1000 IRS solver simulations that show how well the estimated stopping criterion controls the actual residual moving average for three different systems and three sketching methods. The frequency table categories are “Correct” to indicate that either the actual moving average is greater than  $\delta_{II}v$  when  $\rho_k^\lambda > v$  or the actual moving average is less than  $\delta_{II}v$  when  $\rho_k^\lambda \leq v$ , “Below” to indicate when the  $\delta_{II}$  portion of the correct condition is not satisfied, or “Above” to indicate when the  $\delta_{II}$  portion is not satisfied. The left panel and right panel in each pair are  $\eta = 1$  or  $\eta$  as in Table 3, respectively. In all cases, the estimated stopping condition controls the actual residual moving average as we expected.

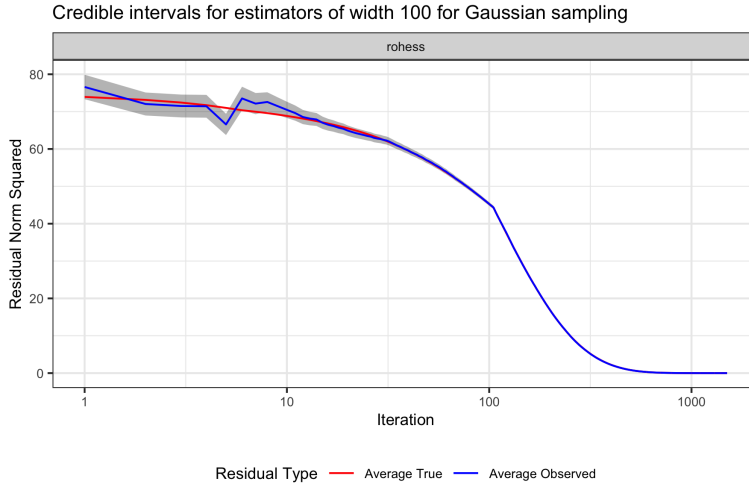


Fig. 6: The estimated 0.95-credible interval covers over 95% of the actual residual moving averages for the square Rohess system of dimension 16,384.

the iterates, an estimator for the aforementioned estimator’s uncertainty set, and an estimated stopping criterion. We rigorously developed these estimators by proving that (1) all moments of the absolute error converge to zero in expectation; (2) the estimates of the moving average of the residual norms squared and to the fourth power are consistent; (3) the estimate of the moving average of the residual norms squared has a sub-Exponential distribution; (4) and by bounding the relative error between  $M_{k-\lambda+1}$  and  $\iota_k^\lambda$  to use the latter as a reasonable plug-in estimator for the former. We then demonstrated the accurate performance of these estimators through

extensive simulations, and demonstrated the capability of our complete algorithm on a problem at scale. Moving forward, we will extend these estimators to iterative random sketching for ordinary least squares problems.

### Appendix A. Supporting theory.

**A.1. Equivalence of  $B$  and 2-norm.** We begin the supplemental material by showing that the  $B$  and 2-norms are equivalent to one another and can be interchanged with only the cost of some constant factor.

LEMMA A.1. *The  $B$  norm is equivalent to the 2-norm with*

$$(A.1) \quad s_n(B)\|x\|_2^2 \leq \|x\|_B^2 \leq s_1(B)\|x\|_2^2.$$

*Proof.* Note,  $s_n(B)I \preceq B \preceq s_1(B)I$ . Therefore, for any  $x$ ,  $s_n(B)\|x\|_2^2 \leq \langle x, Bx \rangle \leq s_1(B)\|x\|_2^2$ . The result follows.  $\square$

**A.2. Bounds on moments of  $S$ .** For the consistency proof of [Theorem 4.6](#) a bound on the 2nd and 4th moments of  $S$  needs to be derived. Given that  $S$  can possibly take uncountably many values, we need a way to impose some finiteness over its behavior. This is the content of the first result.

LEMMA A.2. *There exists a finite set  $\{x_j : j = 1, \dots, b\}$  on the unit sphere such that*

$$(A.2) \quad \mathbb{P} \left( \bigcup_{j=1}^b \{\|S\|_2 \leq 2\|S'x_j\|_2\} \right) = 1.$$

*Proof.* Let  $\mathcal{S}$  denote the unit sphere in  $\mathbb{R}^m$ . Then, by compactness, there exists a finite set of points  $\{x_j : j = 1, \dots, b\}$  such that  $\mathcal{B}(x_j, 1/2) \cap \mathcal{S}$  covers  $\mathcal{S}$ .

Now, there exists a  $y$  with probability one such that  $\|Sy\|_2^2 = \|S\|_2^2$ . For every  $y$ , there exists an  $x \in \{x_j : j = 1, \dots, b\}$  such that  $\|y - x\|_2 \leq 1/2$ . Then, with probability one,

$$(A.3) \quad \|S\|_2 = \|S'y\|_2 \leq \|S'(y - x)\|_2 + \|S'x\|_2 \leq 1/2\|S\|_2 + \|S'x\|_2.$$

Hence,  $\|S\|_2 \leq 2\|S'x\|_2$  for some  $x \in \{x_j : j = 1, \dots, b\}$  with probability one.  $\square$

With this lemma established, we can now progress to bounding the 2nd and 4th moments of  $S$ .

LEMMA A.3. *For  $S$  satisfying the Johnson-Lindenstrauss property (see [Definition 3.3](#)), the second and fourth moments of its largest singular value is bounded.*

*Proof.* We will use the result from [Lemma A.2](#) to get a union bound on the tail probability of the  $d$ th power of the spectral norm of  $S$ .

$$(A.4) \quad \mathbb{P}(\|S\|_2^d > \delta) = \mathbb{P} \left( \|S\|_2 > \delta^{1/d} \right)$$

$$(A.5) \quad \leq \mathbb{P} \left( \bigcup_{i=1}^b \{2\|S'x_i\|_2 > \delta^{1/d}\} \right)$$

$$(A.6) \quad \leq \sum_{i=1}^b \mathbb{P} \left( \|S'x_i\|_2^2 - 1 > \frac{\delta^{2/d} - 4}{4} \right)$$

$$(A.7) \quad \leq 2b \exp \left( - \min \left( \frac{Cp(\delta^{2/d} - 4)}{8\omega}, \frac{Cp(\delta^{2/d} - 4)^2}{16} \right) \right).$$

Using this bound, we can now compute  $\mathbb{E}[\|S\|_2^d]$  using integration by parts.

$$(A.8) \quad \mathbb{E}[\|S'\|_2^d] = \int_0^\infty \mathbb{P}(\|S\|_2^d > \delta) d\delta$$

$$(A.9) \quad = \int_0^{(\sqrt{\frac{2}{\omega}}+2)^d} \mathbb{P}(\|S\|_2^d > \delta) d\delta + \int_{(\sqrt{\frac{2}{\omega}}+2)^d}^\infty \mathbb{P}(\|S\|_2^d > \delta) d\delta$$

$$(A.10) \quad \leq \left(\sqrt{\frac{2}{\omega}}+2\right)^d + 2b \int_{(\sqrt{\frac{2}{\omega}}+2)^d}^\infty \exp\left(-\frac{Cp(\delta^{2/d}-4)}{8\omega}\right) d\delta.$$

The ultimate integral is finite when  $d = 2, 4$ , which gives us the desired result.  $\square$

**A.3. Sub-Exponential Random Variables.** Here, we prove the converse to Proposition 2.9 of [12] in order to verify the claim that Definition 3.3, has a corresponding moment generating function bound.

LEMMA A.4. *Given a centered random variable  $x$  such that*

$$(A.11) \quad \mathbb{P}(|x| > \epsilon) \leq \begin{cases} 2 \exp\left(\frac{-\epsilon^2}{2\sigma^2}\right) & 0 \leq \epsilon \leq \frac{\sigma^2}{\omega} \\ 2 \exp\left(\frac{-\epsilon}{2\omega}\right) & \epsilon \geq \frac{\sigma^2}{\omega} \end{cases},$$

then  $x \sim SE(\sigma^2, \omega)$

*Proof.* From Theorem 2.13 of [12] we have that a distribution is sub-exponential if for all  $\epsilon > 0$  there exists constants  $c_1, c_2$  such that  $\mathbb{P}(|x| \geq \epsilon) \leq c_1 e^{-c_2 \epsilon}$ . Since we know for  $\epsilon \geq \frac{\sigma^2}{\omega}$  we have

$$(A.12) \quad \mathbb{P}(|x| > \epsilon) \leq 2 \exp\left(\frac{-\epsilon}{2\omega}\right)$$

we can select  $c_2 = \frac{1}{2\omega}$ . We can then use this value to selected  $c_1$  such that for  $0 \leq \epsilon \leq \frac{\sigma^2}{\omega}$  we have

$$(A.13) \quad 2 \exp\left(\frac{-\epsilon^2}{2\sigma^2}\right) \leq c_1 e^{-\frac{\epsilon}{2\omega}}.$$

Rearranging this inequality we have to choose  $c_1$  such that for all  $\epsilon > 0$  we have

$$(A.14) \quad 2 \exp\left(\frac{-\epsilon^2}{2\sigma^2} + \frac{\epsilon}{2\omega}\right) < c_1.$$

To select  $c_1$  we will choose it such that (A.14) holds for the  $\epsilon$  that maximizes  $2 \exp\left(\frac{-\epsilon^2}{2\sigma^2} + \frac{\epsilon}{2\omega}\right)$ .  $\blacksquare$

Since this is a smooth function, and we are searching for the maximum over a compact set, by definition of sub-Exponential we know that this maximum exists. Taking derivatives of the exponents and setting them equal to zero gives us the maximizing  $\epsilon = \frac{\sigma^2}{2\omega}$ . Plugging this in to (A.14) we now want to select  $c_1$  such that

$$(A.15) \quad 2 \exp\left(\frac{-\epsilon^2}{2\sigma^2} + \frac{\epsilon}{2\omega}\right) \leq 2 \exp\left(\frac{\sigma^2}{8\omega^2}\right) = c_1.$$

Doing this by construction we have that

$$(A.16) \quad \mathbb{P}(|x| > \epsilon) \leq \begin{cases} 2 \exp\left(\frac{-\epsilon^2}{2\sigma^2}\right) & 0 \leq \epsilon \leq \frac{\sigma^2}{\omega} \\ 2 \exp\left(\frac{-\epsilon}{2\omega}\right) & \epsilon \geq \frac{\sigma^2}{\omega} \end{cases} \leq 2 \exp\left(\frac{\sigma^2}{8\omega^2}\right) \exp\left(\frac{-\epsilon}{2\omega}\right), \quad \square$$

which allows us to conclude that  $x$  is sub-Exponential by Theorem 2.13 of [12].

**A.4. Distribution Constants for Common Sampling Methods.** To be able to use common sampling methods for our estimators, we must compute the constants in the Johnson-Lindenstrauss property (see [Definition 3.3](#)). We will first find the constants for Achlioptas sketching [[1](#)] and Gaussian sketching. Then, we will find constants for FJLT [[2](#)].

**COROLLARY A.5.** *The variance constant for the Gaussian and Achlioptas sampling methods will be*

$$(A.17) \quad 0.23467.$$

*Proof.* Noting from [[1](#)] that for a unit vector  $x$   $\mathbb{P}(\|S'x\|_2^2 > (1 - \epsilon)p/m) \geq \mathbb{P}(\|S'x\|_2^2 > (1 + \epsilon)p/m)$  it is necessary to only bound the tail probability of  $\mathbb{P}(\|S'x\|_2^2 > (1 - \epsilon)p/m)$ . To do this we will find a constant  $C$  such that  $\mathbb{P}(\|S'x\|_2^2 > (1 - \epsilon)p/m) \leq \exp(-\frac{\epsilon^2}{2C})$ . Using equation (16) from [[1](#)] we will have that

$$(A.18) \quad \mathbb{P}(\|S'x\|_2^2 > (1 - \epsilon)p/m) \leq \left(1 + \frac{\epsilon}{2(1 + \epsilon)} + \frac{3\epsilon^2}{8(1 + \epsilon)^2}\right)^k \exp\left(\frac{k\epsilon(1 - \epsilon)}{2(1 + \epsilon)}\right).$$

Thus, we will try to find the  $C$  such that

$$(A.19) \quad \left(1 + \frac{\epsilon}{2(1 + \epsilon)} + \frac{3\epsilon^2}{8(1 + \epsilon)^2}\right)^p \exp\left(\frac{p\epsilon(1 - \epsilon)}{2(1 + \epsilon)}\right) \leq \exp(-Cp\epsilon^2).$$

Taking the log of both sides of [\(A.19\)](#) we have

$$(A.20) \quad p \log\left(1 - \frac{\epsilon}{2(1 + \epsilon)} + \frac{3\epsilon^2}{8(1 + \epsilon)^2}\right) + \frac{p\epsilon(1 - \epsilon)}{2(1 + \epsilon)} \leq -Cp\epsilon^2.$$

Which implies that

$$(A.21) \quad -\log\left(1 - \frac{\epsilon}{2(1 + \epsilon)} + \frac{3\epsilon^2}{8(1 + \epsilon)^2}\right) - \frac{\epsilon(1 - \epsilon)}{(1 + \epsilon)} \geq C\epsilon^2.$$

Which after rearranging will give us that

$$(A.22) \quad C \leq \frac{-2p \log\left(1 - \frac{\epsilon}{2(1 + \epsilon)} + \frac{3\epsilon^2}{8(1 + \epsilon)^2}\right) - \frac{p\epsilon(1 - \epsilon)}{(1 + \epsilon)}}{-\epsilon^2}.$$

Finding a positive local min of the equation on the right-hand side of [\(A.22\)](#) gives us that

$$(A.23) \quad C \leq 0.235467. \quad \square$$

To examine the FJLT case it is necessary to compute the constants from the proof in [[2](#)]. Noting of course that the method proposed in [[2](#)] is not exactly the same as the FJLT, it is based on the same idea and should provide a good enough constant for demonstrative purposes. In order to determine the constants it is necessary to apply lemma 2.3 of [[2](#)].

**LEMMA A.6** (Lemma 2.3 Ailon et al.). *With probability at least  $1 - 1/20n$*

- $q/2 \leq Z_i \leq 2q$  for all  $i = 1, \dots, d$  and
- $dq(1 - \delta) \leq \sum_{i=1}^d Z_i \leq dq(1 + \delta)$

It should be noted that  $q$  is the probability a row is selected.  $Z$  is the sum of the squared elements of the projection residual that are selected by the row sampling.

COROLLARY A.7. *The variance constant for the FJLT will be*

$$(A.24) \quad \frac{1}{32}$$

*Proof.* To get the values to determine the variance it is going to be necessary to first complete the proof of the L2 case from [2]. In order to get the constants on the probability bound. In their proof, it is assumed w.l.o.g that  $\|r_k\|_2^2 = 1$ . From their proof we have

$$(A.25) \quad \mathbb{P} \left[ \|S_{k+1} r_k\| > (1 + \delta) \sum_{i=1}^p Z_i/q \right] \leq \exp \left( -\delta \lambda \sum_{i=1}^d Z_i/q + \xi \lambda^2 \sum_{i=1}^p (Z_i/q)^2 \right).$$

Setting  $\lambda = \frac{\delta \sum_{i=1}^p Z_i/q}{2\xi \sum_{i=1}^p (Z_i/q)^2}$  and plugging it into (A.25) results in

$$(A.26) \quad \mathbb{P} \left[ \sum_{i=1}^p y_i^2 > (1 + \delta) \sum_{i=1}^d Z_i/q \right] \leq \exp \left( -\frac{\delta^2 (\sum_{i=1}^d Z_i/q)^2}{4\xi \sum_{i=1}^p (Z_i/q)^2} \right).$$

Assuming  $\delta$  to be sufficiently small to avoid convergence issues and Using Lemma A.6 we get that

$$(A.27) \quad (A.26) \leq \exp \left( -\frac{p\delta^2}{64\xi} \right).$$

Noting the same size tail estimate can be derived for the left tail we have

$$(A.28) \quad \mathbb{P} \left[ \sum_{i=1}^p y_i^2 > (1 + \delta)k \right] \leq 2 \exp \left( -\frac{p\delta^2}{64\xi} \right).$$

Taking  $\xi = 1$  to ensure convergence, this is exactly the sub-Gaussian part of sub-Exponential tail giving us that

$$(A.29) \quad C = \frac{1}{32}. \quad \square$$

**A.5. Contraction Parameter.** We explore different choices of the contraction parameter,  $\eta$ , and its impact on the reliability of the estimated  $1 - \alpha$  credible interval with  $\alpha = 0.05$ . We experiment with several factors: embedding dimension ( $p$ ), the moving window width ( $\lambda$ ), the sketching method, the system being solved, and the values of the contraction parameter ( $\eta$ ). The embedding dimension is either 25, 50, or 100; the moving average window is either 15, 30 or 100; the three sketching methods are Achlioptas, Gaussian or FJLT; there are several systems that are considered (see supplement Table 6); and the contraction parameter values are allowed to range from 1 to 1000 by an increment of one. For each combination of levels from each factor, we run 1000 simulations, and record the frequency of simulations that exceed their 0.95-credible interval. The results of the experiment are summarized in Figure 7. Conservative choices of  $\eta$  by sampling method, embedding dimension, and moving window width are tabulated in Appendix A.5, and a shorter summary is provided in

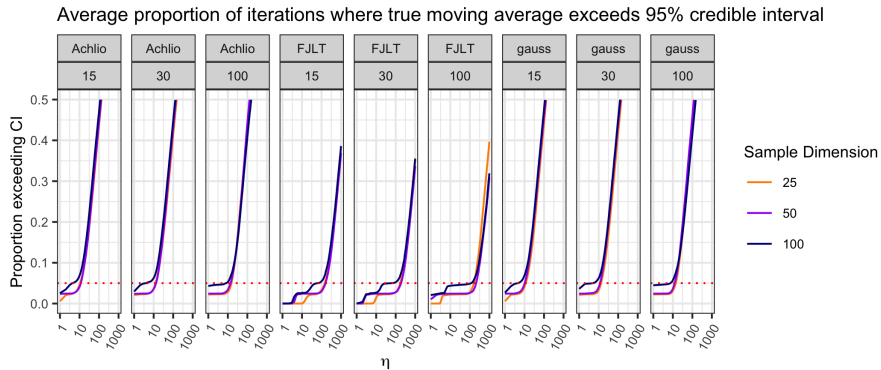


Fig. 7: Percent of iterations where true moving average residual exceeds the 95% credible interval. The graphs are split at different width/sampling method combinations with each color representing a different sampling dimension size. The horizontal dotted line indicates the desired coverage failure of 5%.

Width	Percent Sampled	Achlio	FJLT	gauss
15	0.05	14	192	14
15	0.1	14	212	13
15	0.2	13	188	13
30	0.05	16	213	16
30	0.1	16	248	15
30	0.2	14	221	14
100	0.05	18	199	17
100	0.1	17	264	16
100	0.2	18	255	16

Table 5: Conservative values of the contraction parameter,  $\eta$ , used to achieve credible level at different sample sizes.

**Table 3.** The results for the smallest eta to achieve a failure rate of at least  $\eta$  can be found in [Appendix A.5](#).

**Appendix B. Full table for credible interval experiments.** The results for the failure rates of the credible intervals for systems and sampling methods tested can be found in [Table 6](#). It is important to note that the only matrix with a significant failure rate is the magic matrix and this is believed to be due to numerical errors since all the errors occur when the true residual is on the order of  $10^{-8}$ . The results are also included in [Table 7](#) for the experiment carried out with the appropriate choices of  $\eta$  as defined in [Appendix A.5](#).



Table 6: Frequency of 0.95-credible interval violations by sketching type, coefficient matrix, and true residual level across multiple simulations. Blocks highlighted in red indicate a violation greater than the allowed 0.05 amount.

Sketching	Width	Matrix	Rows	$\eta$	> 10	> $1e-5$	> $1e-10$	> 0	Total
Achlio	100	baart	512	1	0	0	0	0	0
Achlio	100	cauchy	512	1	0	0	0	0	0
Achlio	100	chebspec	512	1	0	0	0	0	0
Achlio	100	chow	512	1	0	0	0	0	0
Achlio	100	circul	512	1	0	0	0	0	0
Achlio	100	deriv2	512	1	0	0	0	0	0
Achlio	100	dingdong	512	1	0	0	0	0	0
Achlio	100	fiedler	512	1	0	0	0	0	0
Achlio	100	foxgood	512	1	0	0	0	0	0
Achlio	100	frank	512	1	0	0	0	0	0
Achlio	100	gilbert	512	1	0	0	0	0	0
Achlio	100	golub	512	1	0	0	0	0	0
Achlio	100	gravity	512	1	0	0	0	0	0
Achlio	100	grcar	512	1	0	0	0	0	0
Achlio	100	hadamard	512	1	0	0	0	0	0
Achlio	100	hankel	512	1	0	0	0	0	0
Achlio	100	heat	512	1	0	0	0	0	0
Achlio	100	hilb	512	1	0	0	0	0	0
Achlio	100	kahan	512	1	0	0	0	0	0
Achlio	100	kms	512	1	0	0	0	0	0
Achlio	100	lehmer	512	1	0	0	0	0	0
Achlio	100	lotkin	512	1	0	0	0	0	0
Achlio	100	magic	512	1	0	0	0.98	0	0.978
Achlio	100	minij	512	1	0	0	0	0	0
Achlio	100	moler	512	1	0	0	0	0	0
Achlio	100	oscillate	512	1	0	0	0	0	0
Achlio	100	parter	512	1	0	0	0	0	0
Achlio	100	pei	512	1	0	0	0	0	0
Achlio	100	phillips	512	1	0	0	0	0	0
Achlio	100	prolate	512	1	0	0	0	0	0
Achlio	100	randcorr	512	1	0	0	0	0	0
Achlio	100	rando	512	1	0	0	0	0	0
Achlio	100	randsvd	512	1	0	0	0	0	0
Achlio	100	rohess	512	1	0	0	0	0	0
Achlio	100	rosser	512	1	0	0	0	0	0
Achlio	100	sampling	512	1	0	0	0	0	0
Achlio	100	shaw	512	1	0	0	0	0	0
Achlio	100	smallworld	512	1	0	0	0	0	0
Achlio	100	spikes	512	1	0	0	0	0	0
Achlio	100	toeplitz	512	1	0	0	0	0	0
Achlio	100	tridiag	512	1	0	0	0	0	0
Achlio	100	triw	512	1	0	0	0	0	0
Achlio	100	ursell	512	1	0	0	0	0	0
Achlio	100	wilkinson	512	1	0	0	0	0	0
FJLT	100	baart	512	1	0	0	0	0	0
FJLT	100	cauchy	512	1	0	0	0	0	0
FJLT	100	chebspec	512	1	0	0	0	0	0
FJLT	100	chow	512	1	0	0	0	0	0
FJLT	100	circul	512	1	0	0	0	0	0
FJLT	100	deriv2	512	1	0	0	0	0	0
FJLT	100	dingdong	512	1	0	0	0	0	0
FJLT	100	fiedler	512	1	0	0	0	0	0
FJLT	100	foxgood	512	1	0	0	0	0	0
FJLT	100	frank	512	1	0	0	0	0	0
FJLT	100	gilbert	512	1	0	0	0	0	0
FJLT	100	golub	512	1	0	0	0	0	0
FJLT	100	gravity	512	1	0	0	0	0	0
FJLT	100	grcar	512	1	0	0	0	0	0
FJLT	100	hadamard	512	1	0	0	0	0	0
FJLT	100	hankel	512	1	0	0	0	0	0
FJLT	100	heat	512	1	0	0	0	0	0
FJLT	100	hilb	512	1	0	0	0	0	0
FJLT	100	kahan	512	1	0	0	0	0	0
FJLT	100	kms	512	1	0	0	0	0	0
FJLT	100	lehmer	512	1	0	0	0	0	0
FJLT	100	lotkin	512	1	0	0	0	0	0
FJLT	100	magic	512	1	0	0	0	0	0
FJLT	100	minij	512	1	0	0	0	0	0
FJLT	100	moler	512	1	0	0	0	0	0
FJLT	100	oscillate	512	1	0	0	0	0	0
FJLT	100	parter	512	1	0	0	0	0	0
FJLT	100	pei	512	1	0	0	0	0	0
FJLT	100	phillips	512	1	0	0	0	0	0
FJLT	100	prolate	512	1	0	0	0	0	0
FJLT	100	randcorr	512	1	0	0	0	0	0
FJLT	100	rando	512	1	0	0	0	0	0
FJLT	100	randsvd	512	1	0	0	0	0	0
FJLT	100	rohess	512	1	0	0	0	0	0
FJLT	100	rosser	512	1	0	0	0	0	0
FJLT	100	sampling	512	1	0	0	0	0	0
FJLT	100	shaw	512	1	0	0	0	0	0
FJLT	100	smallworld	512	1	0	0	0	0	0
FJLT	100	spikes	512	1	0	0	0	0	0
FJLT	100	toeplitz	512	1	0	0	0	0	0
FJLT	100	tridiag	512	1	0	0	0	0	0
FJLT	100	triw	512	1	0	0	0	0	0
FJLT	100	ursell	512	1	0	0	0	0	0
FJLT	100	wilkinson	512	1	0	0	0	0	0
gauss	100	baart	512	1	0	0	0	0	0

gauss	100	cauchy	512	1	0	0	0	0	0
gauss	100	chebspec	512	1	0	0	0	0	0
gauss	100	chow	512	1	0	0	0	0	0
gauss	100	circul	512	1	0	0	0	0	0
gauss	100	deriv2	512	1	0	0	0	0	0
gauss	100	dingdong	512	1	0	0	0	0	0
gauss	100	fiedler	512	1	0	0	0	0	0
gauss	100	foxgood	512	1	0	0	0	0	0
gauss	100	frank	512	1	0	0	0	0	0
gauss	100	gilbert	512	1	0	0	0	0	0
gauss	100	golub	512	1	0	0	0	0	0
gauss	100	gravity	512	1	0	0	0	0	0
gauss	100	grcar	512	1	0	0	0	0	0
gauss	100	hadamard	512	1	0	0	0	0	0
gauss	100	hankel	512	1	0	0	0	0	0
gauss	100	heat	512	1	0	0	0	0	0
gauss	100	hilb	512	1	0	0	0	0	0
gauss	100	kahan	512	1	0	0	0	0	0
gauss	100	kms	512	1	0	0	0	0	0
gauss	100	lehmer	512	1	0	0	0	0	0
gauss	100	lotkin	512	1	0	0	0	0	0
gauss	100	magic	512	1	0	0	0.985	0	0.983
gauss	100	minij	512	1	0	0	0	0	0
gauss	100	moler	512	1	0	0	0	0	0
gauss	100	oscillate	512	1	0	0	0	0	0
gauss	100	parter	512	1	0	0	0	0	0
gauss	100	pei	512	1	0	0	0	0	0
gauss	100	phillips	512	1	0	0	0	0	0
gauss	100	prolate	512	1	0	0	0	0	0
gauss	100	randcorr	512	1	0	0	0	0	0
gauss	100	rando	512	1	0	0	0	0	0
gauss	100	randsvd	512	1	0	0	0	0	0
gauss	100	rohess	512	1	0	0	0	0	0
gauss	100	rosser	512	1	0	0	0	0	0
gauss	100	sampling	512	1	0	0	0	0	0
gauss	100	shaw	512	1	0	0	0	0	0
gauss	100	smallworld	512	1	0	0	0	0	0
gauss	100	spikes	512	1	0	0	0	0	0
gauss	100	toeplitz	512	1	0	0	0	0	0
gauss	100	tridiag	512	1	0	0	0	0	0
gauss	100	triw	512	1	0	0	0	0	0
gauss	100	ursell	512	1	0	0	0	0	0
gauss	100	wilkinson	512	1	0	0	0	0	0

Table 7: Frequency of 0.95-credible interval violations by sketching type, coefficient matrix, true residual level, and contraction parameters ( $\eta$ ) across multiple simulations. Blocks highlighted in red indicate a violation greater than the allowed 0.05 amount.

Sketching	Width	Matrix	Rows	$\eta$	$> 10$	$> 1e-5$	$> 1e-10$	$> 0$	Total
Achlio	100	baart	512	13	0	0	0.001	0	0.001
Achlio	100	cauchy	512	13	0.001	0	0.022	0	0.023
Achlio	100	chebspec	512	13	0	0	0	0	0
Achlio	100	chow	512	13	0	0.038	0	0	0.038
Achlio	100	circul	512	13	0	0	0	0	0
Achlio	100	deriv2	512	13	0	0.001	0	0	0.001
Achlio	100	dingdong	512	13	0.001	0	0	0	0.001
Achlio	100	fiedler	512	13	0.008	0	0	0	0.008
Achlio	100	foxgood	512	13	0	0.001	0.002	0	0.003
Achlio	100	frank	512	13	0	0	0	0	0
Achlio	100	gilbert	512	13	0.002	0	0	0	0.002
Achlio	100	golub	512	13	0	0	0	0	0
Achlio	100	gravity	512	13	0	0.001	0.002	0	0.003
Achlio	100	grcar	512	13	0.001	0.01	0	0	0.011
Achlio	100	hadamard	512	13	0	0	0	0	0
Achlio	100	hankel	512	13	0.013	0	0	0	0.013
Achlio	100	heat	512	13	0	0.061	0	0	0.061
Achlio	100	hilb	512	13	0.001	0	0.013	0	0.014
Achlio	100	kahan	512	13	0	0.014	0	0	0.014
Achlio	100	kms	512	13	0.013	0.022	0	0	0.035
Achlio	100	lehmer	512	13	0	0.028	0	0	0.028
Achlio	100	lotkin	512	13	0	0	0.03	0	0.03
Achlio	100	magic	512	13	0	0.001	0.997	0	0.998
Achlio	100	minij	512	13	0	0.002	0	0	0.002
Achlio	100	moler	512	13	0.002	0	0	0	0.002
Achlio	100	oscillate	512	13	0	0	0	0	0
Achlio	100	parter	512	13	0.002	0	0	0	0.002
Achlio	100	pei	512	13	0	0.004	0.046	0	0.05
Achlio	100	phillips	512	13	0	0.015	0	0	0.015
Achlio	100	prolate	512	13	0.003	0	0	0	0.003
Achlio	100	randcorr	512	13	0.001	0	0	0	0.001
Achlio	100	rando	512	13	0.001	0.006	0	0	0.007
Achlio	100	randsvd	512	13	0	0.005	0	0	0.005
Achlio	100	rohess	512	13	0	0.028	0.005	0	0.033
Achlio	100	rosser	512	13	0	0.046	0	0	0.046
Achlio	100	sampling	512	13	0.03	0	0	0	0.03
Achlio	100	shaw	512	13	0	0	0.105	0	0.105
Achlio	100	smallworld	512	13	0.006	0	0	0	0.006
Achlio	100	spikes	512	13	0	0	0.022	0	0.022
Achlio	100	toeplitz	512	13	0.008	0	0	0	0.008
Achlio	100	tridiag	512	13	0	0.002	0	0	0.002

Achlio	100	triv	512	13	0	0	0	0
Achlio	100	ursell	512	13	0	0.001	0.065	0.066
Achlio	100	wilkinson	512	13	0	0	0	0
FJLT	100	baart	512	188	0.001	0	0.074	0.075
FJLT	100	cauchy	512	188	0	0	0.12	0.12
FJLT	100	chebspec	512	188	0	0	0	0
FJLT	100	chow	512	188	0	0.047	0	0.047
FJLT	100	circul	512	188	0	0	0	0
FJLT	100	deriv2	512	188	0	0.001	0	0.001
FJLT	100	dingdong	512	188	0.001	0	0	0.001
FJLT	100	fiedler	512	188	0.027	0	0	0.027
FJLT	100	foxgood	512	188	0	0.001	0.105	0.106
FJLT	100	frank	512	188	0.004	0	0	0.004
FJLT	100	gilbert	512	188	0.001	0.009	0	0.01
FJLT	100	golub	512	188	0	0	0	0
FJLT	100	gravity	512	188	0.001	0	0.024	0.025
FJLT	100	grcar	512	188	0.004	0.076	0	0.08
FJLT	100	hadamard	512	188	0.027	0.018	0.013	0.058
FJLT	100	hankel	512	188	0	0	0	0
FJLT	100	heat	512	188	0	0.008	0	0.008
FJLT	100	hilb	512	188	0	0	0.089	0.089
FJLT	100	kahan	512	188	0	0.109	0	0.109
FJLT	100	kms	512	188	0.002	0	0	0.002
FJLT	100	lehmer	512	188	0	0.001	0	0.001
FJLT	100	lotkin	512	188	0	0.001	0.125	0.126
FJLT	100	magic	512	188	0	0	0.998	0.998
FJLT	100	minij	512	188	0.009	0.03	0	0.039
FJLT	100	moler	512	188	0.107	0	0	0.107
FJLT	100	oscillate	512	188	0	0.014	0	0.014
FJLT	100	parter	512	188	0	0.005	0	0.005
FJLT	100	pei	512	188	0	0.003	0.003	0.006
FJLT	100	phillips	512	188	0.001	0.053	0	0.054
FJLT	100	prolate	512	188	0.01	0.074	0	0.084
FJLT	100	randcorr	512	188	0	0.007	0	0.007
FJLT	100	rando	512	188	0.027	0.024	0	0.051
FJLT	100	randsvd	512	188	0	0.054	0	0.054
FJLT	100	rohess	512	188	0.001	0.021	0.001	0.023
FJLT	100	rosser	512	188	0.068	0.039	0	0.107
FJLT	100	sampling	512	188	0.042	0	0	0.042
FJLT	100	shaw	512	188	0.001	0	0.023	0.024
FJLT	100	smallworld	512	188	0.002	0.027	0	0.029
FJLT	100	spikes	512	188	0	0	0.083	0.083
FJLT	100	toeplitz	512	188	0.027	0	0	0.027
FJLT	100	tridiag	512	188	0	0.056	0	0.056
FJLT	100	triv	512	188	0	0	0	0
FJLT	100	ursell	512	188	0	0	0.09	0.09
FJLT	100	wilkinson	512	188	0.059	0	0	0.059
gauss	100	baart	512	13	0.001	0	0.001	0.002
gauss	100	cauchy	512	13	0	0	0.079	0.079
gauss	100	chebspec	512	13	0	0	0	0
gauss	100	chow	512	13	0.002	0.035	0	0.037
gauss	100	circul	512	13	0	0	0	0
gauss	100	deriv2	512	13	0	0.007	0	0.007
gauss	100	dingdong	512	13	0.001	0.016	0	0.017
gauss	100	fiedler	512	13	0.082	0	0	0.082
gauss	100	foxgood	512	13	0	0.002	0	0.002
gauss	100	frank	512	13	0	0	0	0
gauss	100	gilbert	512	13	0.001	0.04	0	0.041
gauss	100	golub	512	13	0	0	0	0
gauss	100	gravity	512	13	0	0.001	0	0.001
gauss	100	grcar	512	13	0.001	0.001	0	0.002
gauss	100	hadamard	512	13	0	0.008	0	0.008
gauss	100	hankel	512	13	0.006	0	0	0.006
gauss	100	heat	512	13	0	0.001	0	0.001
gauss	100	hilb	512	13	0	0	0.036	0.036
gauss	100	kahan	512	13	0	0.012	0	0.012
gauss	100	kms	512	13	0.003	0.019	0	0.022
gauss	100	lehmer	512	13	0	0.041	0	0.041
gauss	100	lotkin	512	13	0	0	0.006	0.006
gauss	100	magic	512	13	0	0	0.997	0.997
gauss	100	minij	512	13	0.001	0.03	0	0.031
gauss	100	moler	512	13	0.029	0	0	0.029
gauss	100	oscillate	512	13	0	0.009	0	0.009
gauss	100	parter	512	13	0	0.028	0	0.028
gauss	100	pei	512	13	0	0.107	0	0.107
gauss	100	phillips	512	13	0	0.005	0	0.005
gauss	100	prolate	512	13	0	0.009	0	0.009
gauss	100	randcorr	512	13	0.001	0	0	0.001
gauss	100	rando	512	13	0.003	0	0	0.003
gauss	100	randsvd	512	13	0	0.052	0	0.052
gauss	100	rohess	512	13	0.001	0.023	0	0.024
gauss	100	rosser	512	13	0.001	0	0	0.001
gauss	100	sampling	512	13	0.009	0	0	0.009
gauss	100	shaw	512	13	0	0.001	0.001	0.002
gauss	100	smallworld	512	13	0.001	0.006	0	0.007
gauss	100	spikes	512	13	0	0	0.005	0.005
gauss	100	toeplitz	512	13	0.082	0	0	0.082
gauss	100	tridiag	512	13	0	0	0	0
gauss	100	triv	512	13	0.002	0.009	0	0.011
gauss	100	ursell	512	13	0	0	0	0
gauss	100	wilkinson	512	13	0.103	0	0	0.103

**Appendix C. Full stopping error results.** The results for the Achlio and FJLT sampling methods for the three matrix types of subsection 5.3 are displayed below. They show that the  $\iota_k^\lambda$  condition performs equally as well at controlling stopping

errors as in the Gaussian case.

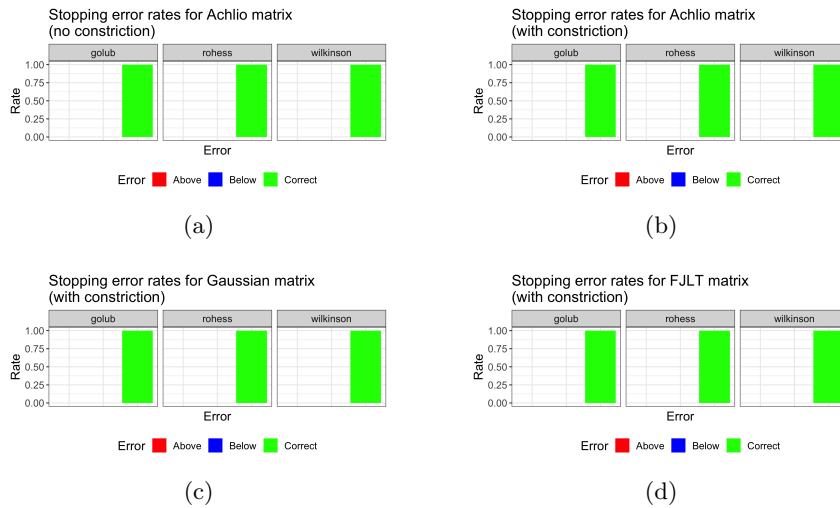


Fig. 8: Frequency tables for 1000 IRS solver simulations that show how well the estimated stopping criterion controls the actual residual moving average for three different systems and three sketching methods. The frequency table categories are “Correct” to indicate that either the actual moving average is greater than  $\delta_{IV}$  when  $\rho_k^\lambda > v$  or the actual moving average is less than  $\delta_{II}v$  when  $\rho_k^\lambda \leq v$ , “Below” to indicate when the  $\delta_I$  portion of the correct condition is not satisfied, or “Above” to indicate when the  $\delta_{II}$  portion is not satisfied. The left panel and right panel in each pair are  $\eta = 1$  or  $\eta$  as in Table 3, respectively. In all cases, the estimated stopping condition controls the actual residual moving average as we expected.

## REFERENCES

- [1] D. ACHLIOPTAS, *Database-friendly random projections: Johnson-lindenstrauss with binary coins*, Journal of Computer and System Sciences, 66 (2003), pp. 671–687, [https://doi.org/https://doi.org/10.1016/S0022-0000\(03\)00025-4](https://doi.org/https://doi.org/10.1016/S0022-0000(03)00025-4), <https://www.sciencedirect.com/science/article/pii/S0022000003000254>. Special Issue on PODS 2001.
- [2] N. AILON AND B. CHAZELLE, *The fast johnson–lindenstrauss transform and approximate nearest neighbors*, SIAM J. Comput., 39 (2009), pp. 302–322.
- [3] S. DASGUPTA AND A. GUPTA, *An elementary proof of a theorem of johnson and lindenstrauss*, Random Struct. Algorithms, 22 (2003), pp. 60–65.
- [4] R. DURRETT, *Probability: Theory and examples*, 2013.
- [5] R. M. GOWER AND P. RICHTÁRIK, *Randomized iterative methods for linear systems*, SIAM Journal on Matrix Analysis and Applications, 36 (2015), p. 1660–1690, <https://doi.org/10.1137/15m1025487>, <http://dx.doi.org/10.1137/15M1025487>.
- [6] P. INDYK AND R. MOTWANI, *Approximate nearest neighbors: Towards removing the curse of dimensionality*, (1998), p. 604–613, <https://doi.org/10.1145/276698.276876>, <https://doi.org/10.1145/276698.276876>.
- [7] W. JOHNSON AND J. LINDENSTRAUSS, *Extensions of lipschitz maps into a hilbert space*, Contemporary Mathematics, 26 (1984), pp. 189–206, <https://doi.org/10.1090/conm/026/737400>.
- [8] J. MATOUŠEK, *On variants of the johnson–lindenstrauss lemma*, Random Structures & Algorithms, 33 (2008), pp. 142–156.
- [9] V. PATEL, M. JAHANGOSHAHI, AND D. A. MALDONADO, *An implicit representation and iterative solution of randomly sketched linear systems*, SIAM Journal on Matrix Analysis and

- Applications, 42 (2021), pp. 800–831.
- [10] M. PILANCI AND M. J. WAINWRIGHT, *Randomized sketches of convex programs with sharp guarantees*, IEEE Transactions on Information Theory, 61 (2015), pp. 5096–5115, <https://doi.org/10.1109/TIT.2015.2450722>.
  - [11] P. RICHTÁRIK AND M. TAKÁČ, *Stochastic reformulations of linear systems: Algorithms and convergence theory*, SIAM Journal on Matrix Analysis and Applications, 41 (2017), <https://doi.org/10.1137/18M1179249>.
  - [12] M. J. WAINWRIGHT, *High-Dimensional Statistics: A Non-Asymptotic Viewpoint*, Cambridge Series in Statistical and Probabilistic Mathematics, Cambridge University Press, 2019, <https://doi.org/10.1017/9781108627771>.
  - [13] W. ZHANG AND N. HIGHAM, *Matrix depot: An extensible test matrix collection for julia*, PeerJ Computer Science, 2 (2016), p. e58, <https://doi.org/10.7717/peerj-cs.58>.